Nano Research

Open Access

Review Article

Full-color micro-LED displays based on quantum dot color converters

Yingqi Zeng[1,§], Wenzhuo Qian[1,§], Rui Long[1], Xiang Zhang[2], Fuqiang Ma[3], Jiajun Luo[2], Linyuan Lian[4] ✉, Daoli Zhang[1,2] ✉, and Jianbing Zhang[1,2] ✉

[1] School of Integrated Circuits, Huazhong University of Science and Technology (HUST), Wuhan 430074, China
[2] Wuhan National Laboratory for Optoelectronics (WNLO), Huazhong University of Science and Technology (HUST), Wuhan 430074, China
[3] Weichai Power Co., Ltd., Weifang 261061, China
[4] Key Laboratory of Materials Physics of Ministry of Education, School of Physics and Microelectronics, Zhengzhou University, Zhengzhou 450052, China
§ Yingqi Zeng and Wenzhuo Qian contribute equally to this work.

Cite this article: *Nano Research*, **2025**, *18*, 94907390. https://doi.org/10.26599/NR.2025.94907390

ABSTRACT: Micro-light-emitting diodes (micro-LEDs) have emerged as a promising display technology featuring high resolution, wide color gamut, high contrast, flexibility, and long lifetime. However, there are severe challenges in full-color micro-LED, such as low efficiencies of red and green micro-LEDs, complex driving circuits for three-color micro-LEDs, and challenging mass transfer. Thus, converting blue light into red and green light by coupling color converters with blue LEDs is a reasonable strategy. Colloidal quantum dots (QDs) are an optimal candidate for color converters due to their high photoluminescence quantum yield, narrow emission peaks, small particle sizes, and solution processibility. Therefore, full-color micro-LEDs based on quantum dot color converters are attracting increasing attention. This review introduces micro-LED technology and the research progress of the full-color realization, and describes the associated technical challenges. Furthermore, it outlines the properties of QDs, patterning techniques, integration with micro-LEDs for achieving full color, and finally analyzes the challenges of applying QDs to micro-LEDs, demonstrating the application potential of QDs in achieving full-color of micro-LEDs, along with prospects for addressing current challenges.

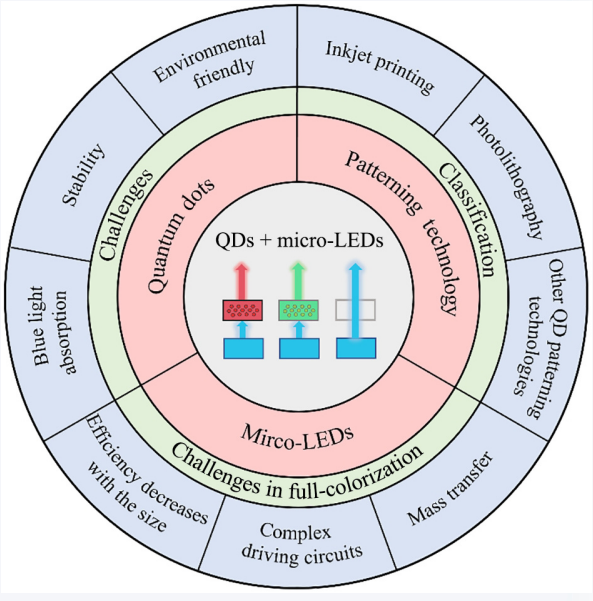

KEYWORDS: micro-light-emitting diode (micro-LED), quantum dot, patterning technology, full-color, color converter

1 Introduction of micro-light-emitting diode (micro-LED)

With the continuous improvement of manufacturing technology, display chips are increasingly developing in the direction of miniaturization. In addition to the current mainstream liquid crystal display (LCD) and organic light-emitting diode (OLED) displays, mini-light-emitting diodes (mini-LEDs) and micro-LEDs have emerged as a new generation of display technology. Micro-LEDs are typically less than 50 μm and rely on a single independent pixel to realize self-illumination to control the display effect, which do not have structures such as liquid crystals and backlight panels. The display panel typically comprises numerous independent micro-LED units transferred to the driver circuit substrate. Therefore, micro-LEDs are thin and can achieve flexible displays. Moreover, they have high resolutions, wide color gamuts, high contrast, great stability, and prolonged lifespan, integrating the advantages of mainstream display technologies [1–4]. Numerous excellent

Received: January 24, 2025; **Revised:** March 18, 2025
Accepted: March 19, 2025

✉Address correspondence to Linyuan Lian, lianlinyuan@zzu.edu.cn; Daoli Zhang, zhang_daoli@hust.edu.cn; Jianbing Zhang, jbzhang@hust.edu.cn

characteristics significantly broaden the application scope of micro-LEDs. For instance, a high Pixel Per Inch (PPI) is imperative for augmented reality/virtual reality (AR/VR) displays. Micro-LEDs not only meet this criterion but also offer additional performance advantages [5], making them a preferred choice for AR/VR displays [6]. What's more, high contrast and color reproduction qualities render them suitable for outdoor and semi-outdoor display scenes such as in-vehicle displays. The independent design of the LED unit allows micro-LED to be flexible in size, which can not only realize large-screen display but also produce curved screens [7]. Furthermore, micro-LEDs are also applied in diverse fields including biological [8, 9] and optical communications [10, 11], etc.

The history of micro-LED can be traced back to 2000, when Jiang's group reported the micro-LED display technology, put forward the relevant concepts and structural schematics [12], and triggered the micro-LED research boom. In terms of full-color realization, in 2011, Liu et al. used red, green, and blue phosphors as the color converting materials for ultraviolet (UV) lights to realize a full-color display of micro-LEDs [13]. In 2013, Liu et al. used a trichroic prism to combine the light from the three light emitting diodes on silicon (LEDoS) chips and prepared a full-color de-backlighted micro-LED projector, which has fewer optical components and high light utilization compared to the traditional projected structure [14]. In 2015, Han et al. used aerosol jet printing technology to achieve a full-color display of micro-LEDs by spraying quantum dots (QDs) on UV micro-LED arrays and using UV light to excite red, green, and blue QDs to achieve full-color, and also using distributed Bragg reflectors (DBRs) to enhance the utilization of UV light [15], Additionally, in 2017, they used photoresist molds to address the optical crosstalk issue [16]. In 2018 Chen et al. combined hybrid Bragg reflector (HBR), DBR, and black matrix simultaneously to further improve the color purity [17]. In 2019, Kuo's group achieved a full-color display in combination with QDs by constructing a nanoring (NR) structure and adjusting the width of the NR-micro-LED [18]. In 2020, Hsiang et al. designed a cholesteric liquid crystal (CLC) polymer film to enhance the color conversion efficiency (CCE) of QDs, increasing the CCE of the display system by about 143% [19]. The development history of micro-LED full-colorization is shown in Fig. 1. These achievements reflect that QDs show great potential for development in micro-LED full-colorization applications.

2 Challenges in full-colorization of micro-LEDs

Although micro-LED has many advantages, there are still many challenges in achieving its full-color display. In the field of direct display, the prevalent method for achieving full-colorization involves using III-V compound semiconductors to produce the three primary colors: red, green, and blue (RGB). The three-color LEDs are arranged on the substrate in sequence, and single-color control is achieved through different bias voltages. However, this full-colorization method has the following challenges.

2.1 The efficiency of red and green micro-LEDs decreases significantly as their size is reduced

Micro-LED devices are typically manufactured through the dry etching of LED films. As the chip size decreases, inductively coupled plasma etching causes damage to the sidewalls of the micro-LED chip during the device fabrication, which results in an increased ratio of the damaged area to the active area, leading to a rise in defects and subsequently more Shockley-Read-Hall (SRH) non-radiative recombination and requiring higher current densities to achieve peak internal quantum efficiency (IQE) [22–25]. Furthermore, as the size of LEDs continues to decrease, the luminous efficiency also decreases to varying degrees. For InGaN semiconductors, longer wavelength quantum wells (QWs) require higher indium content and lower growth temperatures. The increase in indium content leads to the generation of a strong polarization field in multiple quantum wells (MQWs), resulting in a pronounced quantum-confined Stark effect, which reduces the

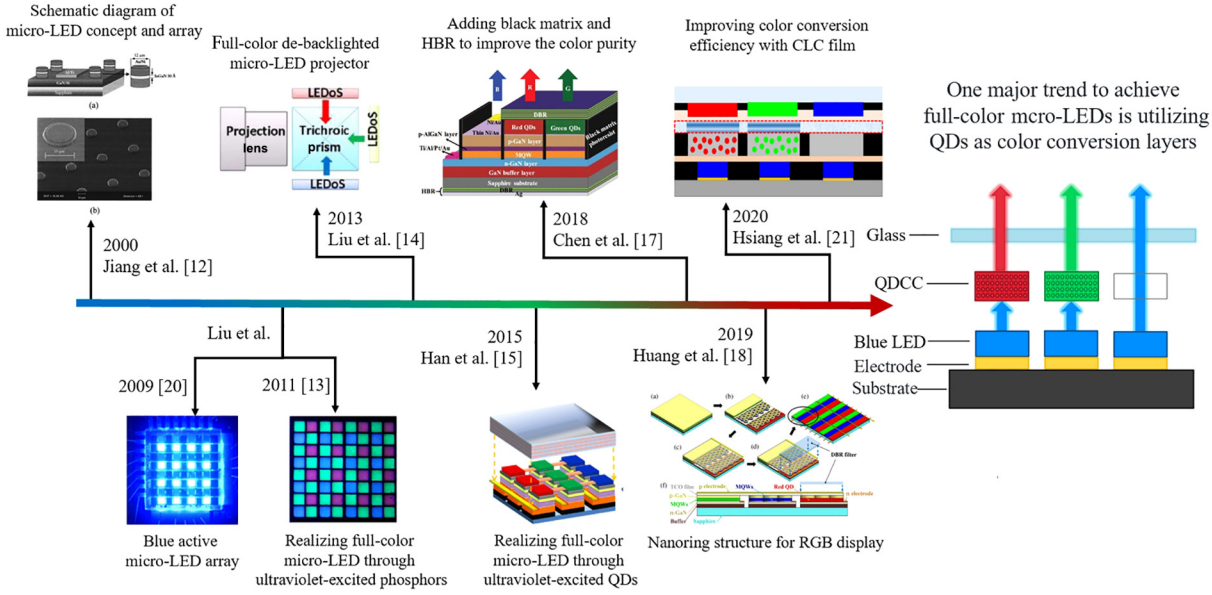

Figure 1 Micro-LED full-color development history. First row of images, left to right: reproduced with permission from Ref. [12], © AIP Publishing 2000; reproduced with permission from Ref. [14], © IEEE 2013; reproduced with permission from Ref. [17], © IEEE 2018; reproduced with permission from Ref. [20], © Society for Information Display 2021. Second row of images, left to right: reproduced with permission from Ref. [21], © IEEE 2009; reproduced with permission from Ref. [13], © Society for Information Display 2011; reproduced with permission from Ref. [15], © Optical Society of America 2015; reproduced with permission from Ref. [18], © Chinese Laser Press 2019.

recombination efficiency and forms more dislocations, point defects, and severe phase segregation, ultimately causing an increase in non-radiative recombination and a decrease in efficiency [26, 27]. Consequently, the luminescence efficiency of green LEDs is low. Furthermore, for red LEDs, due to the high surface recombination rate and long carrier diffusion length of AlGaInP micro-LEDs [28, 29], the luminescence efficiency decreases even more severely as the size decreases. Typically, the external quantum efficiency of red and green LEDs is lower than that of blue LEDs of the same size, as depicted in Fig. 2 [7].

2.2 Driving circuits are complex

For LEDs of different colors, their threshold voltages are different (approximately 3.3 V for blue LEDs, 1.7 V for red LEDs and 2.2 V for green LEDs). Additionally, the performance of LEDs made of different materials varies in the same environment, which needs to be considered separately when designing the driving circuit, increasing the complexity of the circuit [30].

2.3 Mass transfer is a big challenge

To integrate individual micro-LEDs into a display panel, a mass transfer process is usually required. Mass transfer refers to growing chips on a substrate, then separating a large number of micro-LED chips from the source substrate and transferring them onto a target substrate or driver circuit board. Mainstream mass transfer techniques include pick-and-place transfer [31–35], roll-to-roll transfer [36], fluidic self-assembly transfer [37–39], laser-assisted lift-off transfer [40–44], and chemical bonding technology [45]. For large-screen displays, there are a large number of micro-LED chips. For example, for an 8K display, the number of chips can even reach hundreds of millions. Therefore, the transfer speed requirement is very high. In order to ensure correct interconnection, the transfer accuracy is usually required to be within ±1 μm [46], and the industry's yield requirement is > 99.9999%. However, due to the extremely small size of micro-LED, it is very difficult to achieve accurate grasping and positioning. In addition, micro-LED chips are very fragile and easily damaged during the transfer process. Moreover, the mass transfer of three colors of micro-LEDs in sequence, as shown in Fig. 3(a), further increases the difficulty.

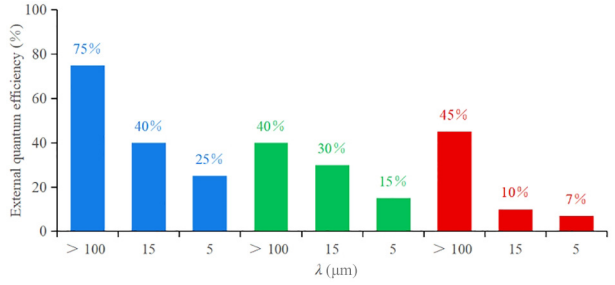

Figure 2 Comparison of the decrease in external quantum efficiency of RGB LEDs with the reduction of chip size. Reproduced with permission from Ref. [7], © Nanjing Electronic Devices Institute 2023.

Full-color micro-LEDs based on color converters are a promising strategy to avoid the above challenges. To address the aforementioned issues, full colorization can be achieved by combining with a quantum dot color converter (QDCC). In this approach, the color conversion material is deposited onto the monochromatic blue LED, and the red and green colors are realized by exciting the color conversion materials with blue light as shown in Fig. 3(b). In this way, only blue LEDs are mass transferred, thereby reducing engineering complexity and only one type of driving circuit is needed. Common color conversion materials include phosphor and QDs, etc. Traditional phosphors are widespread and cost-effective, offering high thermal and chemical stabilities [47], making them commonly used in daily lighting [1]. However, they have a broad yellow emission spectrum, large particle sizes, and coating thicknesses [48], which leads to uneven color deposition and pixel crosstalk when applied to small-sized pixels such as micro-LEDs. Additionally, the small absorption cross-section of traditional phosphors limits their effectiveness in absorbing blue light, which in turn affects the CCE [49]. In contrast, QDs have dimensions at the nanometer scale [50], making them more suitable for application to micro-LED displays. Furthermore, QDs exhibit several outstanding optoelectronic properties, which will be described in detail below, and demonstrate their combination with micro-LEDs. Table 1 compares the characteristics of QDs with other emitting materials (such as organic fluorescent materials and inorganic phosphors) in the applications of micro-LEDs.

3 Application of quantum dots in micro-LEDs

3.1 Introduction of QDs

QDs are semiconductor nanocrystals synthesized by wet chemical methods [50]. In QDs, the exciton Bohr radius is confined by the size, differing from that at macroscopic scales. This confinement prevents the electrons and holes in QDs from forming collective motion or quasi-continuous conduction and valence bands, resulting in discrete quantized energy levels rather than a

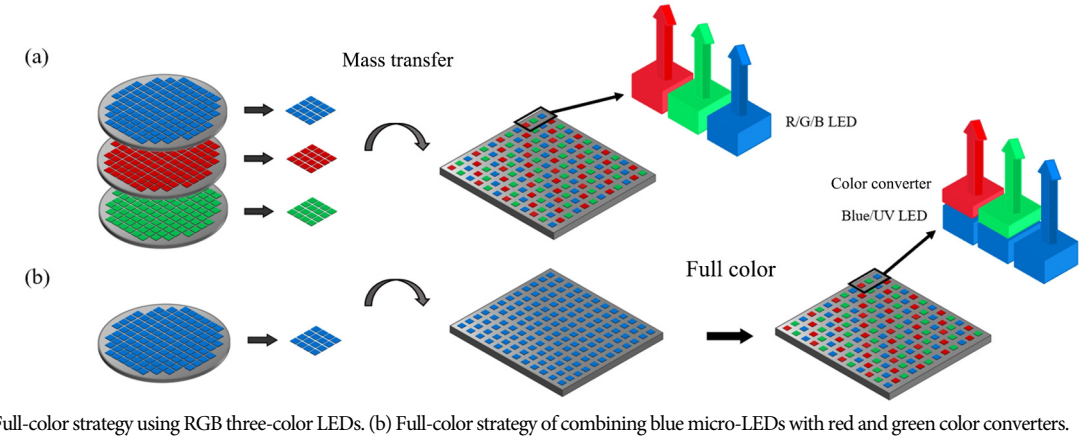

Figure 3 (a) Full-color strategy using RGB three-color LEDs. (b) Full-color strategy of combining blue micro-LEDs with red and green color converters.

Table 1 Performance comparison of QDs with other emitting materials

Performance metric	Quantum dots	Organic fluorescent material	Phosphors
Wavelength tunability	High	Low	Low
Color purity	High	Medium	Low
Stability	High	Low	High
Fabrication process	Solution	Vacuum or solution	High-temperature sintering
Pixel uniformity	High	High	Low
Particle size	Small	Small	Large
Absorption coefficient	High	Medium	Low

continuous band structure. Typically, the bandgap of a QD increases as its size decreases due to the quantum confinement effect, rendering it adjustable. Consequently, QDs with different bandgaps emit light of corresponding wavelengths. By flexibly adjusting the QD size, any desired luminescence wavelength can be achieved [51–54]. Typically, QDs are composed of a core-shell structure as well as external ligands, which significantly influence their properties. These ligands reside on the high surface area of QDs and make passivation of QDs, confining carriers within the core and enhancing optical characteristics. With a narrow light-emitting half-peak width of approximately 20–30 nm, QDs produce high-purity monochromatic light. This allows it to display richer and more accurate color representation across a broader gamut, meeting the demands of applications requiring superior color performance in displays. Moreover, QDs can be synthesized at a low cost using a straightforward solution method, which is easy to mass-produce. And they are compatible with various substrates [55]. With these exceptional characteristics, QDs find extensive applications in LED displays as color converting materials, enhancing color gamut and brightness [56]. For the application of QDs in micro-LED, the QDs need to be patterned to couple with the blue LED array.

3.2 Quantum dot patterning technique

The patterning of the QDCC in micro-LEDs presents a significant technical challenge in achieving high-resolution full-color displays. This necessitates the accurate patterning of red and green colors within each micro-LED pixel and the integration or encapsulation of the color converter with blue LED arrays to form a functional device. Therefore, it is essential to develop techniques for fabricating micrometer-scale patterns of QDs with different light-emitting colors [57]. In the process of patterning the QDCC, it is necessary to consider the compatibility between different materials, improve the effective absorption and conversion efficiency of the QDCC for blue LEDs, and ensure the optical and thermal stability of the QD material and the entire LED array when working in an integrated manner. Current research progress indicates that patterning techniques for QDCC include inkjet printing [58], photolithography [59], transfer printing [60], etc. These studies provide various promising patterning methods for the preparation of QDCC, thereby providing robust support for advancements in this field.

3.2.1 Inkjet printing

Inkjet printing technology stands as the current mainstream QD patterning technique, including aerosol jet printing (AJP) and electrohydrodynamic (EHD) jet printing. The principle is to spray ink dissolved with red, green, or blue QDs through nozzles to form the desired pattern via precise spraying onto the substrate [61, 62]. QDs are typically synthesized via solution methods, which are highly process-compatible with inkjet printing technology, having the advantages of low cost, non-contact application, and minimal material loss.

Conventional inkjet printing is limited by the nozzle size and the viscosity of the ink, which restricts its ability to prepare QDCCs with high pixel density. In the quest for more precise and smaller-scale QD patterning methods, AJP and EHD printing have emerged [63–65]. AJP employs ultrasonic or pneumatic atomization to convert ink into minute droplets, and then the ink is transferred to the substrate via high-pressure airflow, as depicted in Fig. 4(a). In 2015, Kuo's group utilized AJP to deposit red, green, and blue QDs onto the surfaces of UV micro-LED arrays and successfully fabricated a QD full-color micro-LED array featured with a pixel size of 40 μm, and a luminous efficiency of 32 $lm \cdot W^{-1}$. However, there was an optical crosstalk problem between its adjacent QD pixels [15]. Building upon this work, in 2017, they introduced a black photoresist and employed photolithography to create a 35 μm × 35 μm black matrix serving as an enclosing dam. Subsequently, red, green, and blue QDs were individually injected into the matrix. The integration of the black matrix effectively constrained the QD ink to fixed positions, significantly reducing optical crosstalk between neighboring pixels. The crosstalk rate was reduced from 32.8% to almost 0 compared to the previous device without the black matrix. Furthermore, a DBR centered at 395 nm was incorporated to optimize the UV micro-LEDs' absorption and conversion, further enhancing the device's luminescence intensity [16].

EHD printing uses electric field forces to drive the deposition of QD ink droplets onto the substrate, which is not limited by the nozzle diameter and can further improve the precision of QD patterning [67]. During printing, a small amount of free charge exists in the solution at the nozzle, which, in the presence of an electric field, is collected at the gas-liquid interface, subjecting it to normal and tangential electric field forces, as demonstrated in Fig. 4(c). Consequently, under the force, the liquid tip at the nozzle deforms, forming a Taylor cone and ejecting fine jets to deposit the QD ink droplets onto the substrate, which can be controlled to achieve submicron accuracy in QD patterning [68].

However, a common issue of EHD printing and AJP is that the QDCC forms unevenly during the evaporation and drying process of QD ink, known as the coffee-ring effect [69]. Due to the specific viscosity and wettability of QD ink, the edge of the droplet deposited on the substrate exhibits a thinner thickness compared to the center. Consequently, the evaporation rate at the droplet edge surpasses that of the center, leading to the formation of capillary flow within the droplet induced by surface tension and capillarity. This flow transports the QD particles to the edge, ultimately resulting in an uneven pattern similar to a coffee ring, which adversely affects the final display quality. To solve this problem, Li et al. prepared high-resolution pixel dot arrays with a diameter of 1 μm by optimizing and improving the solvent of the QD ink by EHD printing, as shown in Fig. 4(d), the coffee-ring effect can be effectively suppressed by controlling the volume ratio of cyclohexylbenzene (CHB) to nonane at 8:2 in the mixed solvent [66]. The coffee-ring effect can also be suppressed by introducing a black matrix as an enclosing dam, as shown in Fig. 4(b), where a black photoresist mold is designed to match the height of the QD

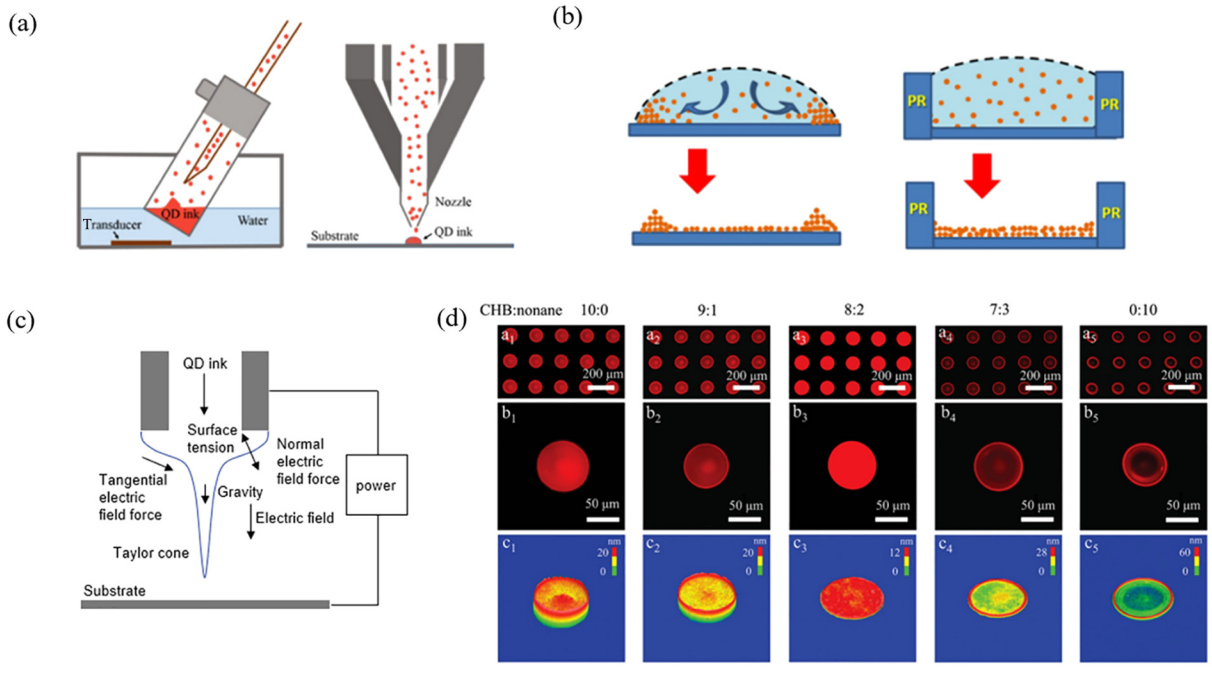

Figure 4 (a) Schematic diagram of aerosol spraying. Reproduced with permission from Ref. [15], © Optical Society of America 2015. (b) Introduction of photoresist surround dam to suppress the coffee ring effect. Reproduced with permission from Ref. [16], © Chinese Laser Press 2017. (c) Schematic diagram of EHD printing. (d) Adjustment of solvent ratio to suppress the coffee ring effect. Reproduced with permission from Ref. [66], © WILEY-VCH Verlag GmbH & Co. KGaA, Weinheim 2020.

ink droplet, ensuring similar liquid thicknesses at both the edges and in the middle of the droplet. Maintaining uniform liquid thicknesses results in comparable evaporation rates, thereby preventing the capillary flow induced by evaporation from transporting QDs to the edge [16].

In summary, inkjet printing technology offers a broad application scope in the QD patterning process owing to its advantages of controllable process, simple method, low cost, non-contact, and high material utilization. Emphasis is placed on manipulating the physical properties of QD ink and enhancing the precision and productivity of printing equipment. In scenarios such as micro-LED display manufacturing, which demands mass production of high-resolution panels (like the common 1080P (1920 × 1080) resolution, which requires millions of pixel points with uniformity), posing a significant current challenge for inkjet printing technology.

3.2.2 *Photolithography*

Photolithography stands also as one of the prevailing techniques for QD patterning, including the photolithographic lift-off process, sacrificial layer-assisted lithography, photosensitive ligand-assisted lithography, and hybrid QD and photoresist lithography schemes [70–72]. The fundamental principles can be categorized into two types. One is to use a photoresist to create a mold or mask for QD patterning via photolithography, and then fill or remove the designated area of QDs to form the patterning; the other method involves engineering QD materials with photosensitive ligands on the surface, and then directly form the QD patterns through photolithography process [73]. Compared with inkjet printing technology, photolithography can achieve ultra-high-precision QD patterns and is highly compatibility with existing semiconductor fabrication processes, rendering it suitable for large-scale production.

In 2016, Park et al. prepared full-color QD patterns with a sub-pixel size of 10 μm × 40 μm using a photolithographic lift-off process that combines conventional lithography with charge-assisted layer-by-layer (LbL) deposition technique [71]. Photoresist mask patterns were created on Si(100) wafers with a 1 μm thickness of SiO_2 on the surface using a conventional lithography process, and the photoresist surface was charged via plasma treatment. Subsequently, a layer of red QDs was deposited on the surface, and the photoresist layer was subsequently peeled off by immersion in acetone and methanol and ultrasonic cleaning, respectively, to obtain patterned red QDs, as depicted in Fig. 5(a). Through repetition of the aforementioned process, red, green, and blue QD patterns can be prepared, yielding a pixelated full-color QD layer. However, the photolithographic lift-off process requires multiple removals of the photoresist mask pattern, resulting in issues such as incomplete removal of the photoresist and potential damage to the QDs within the patterned region [74]. To reduce the damage to the QD layer from the photolithographic lift-off process, BOE Technology Group proposed to prepare the pattern of the QDCC with the assistance of a negative photoresist and a sacrificial layer. The introduction of the sacrificial layer maintains the integrity of the QD layer and facilitates the removal of the photoresist. Initially, a sacrificial layer of polyvinylpyrrolidone (PVP) was applied onto the substrate, then photoresist was spin-coated on the sacrificial layer. Subsequently, the sacrificial layer in the patterned region was removed through inductively coupled plasma etching after exposure and development of the pattern, and then deposited QDs. This process effectively separates the QD layer from the photoresist layer within the patterned area, enabling straightforward removal of the sacrificial layer when peeling off the photoresist, thus minimizing damage to the QD pattern [75]. In 2019, Kim et al. mixed QDs with photoresists for lithography. They used a solvent called propylene glycol monomethyl ether acetate (PGMEA) to mix

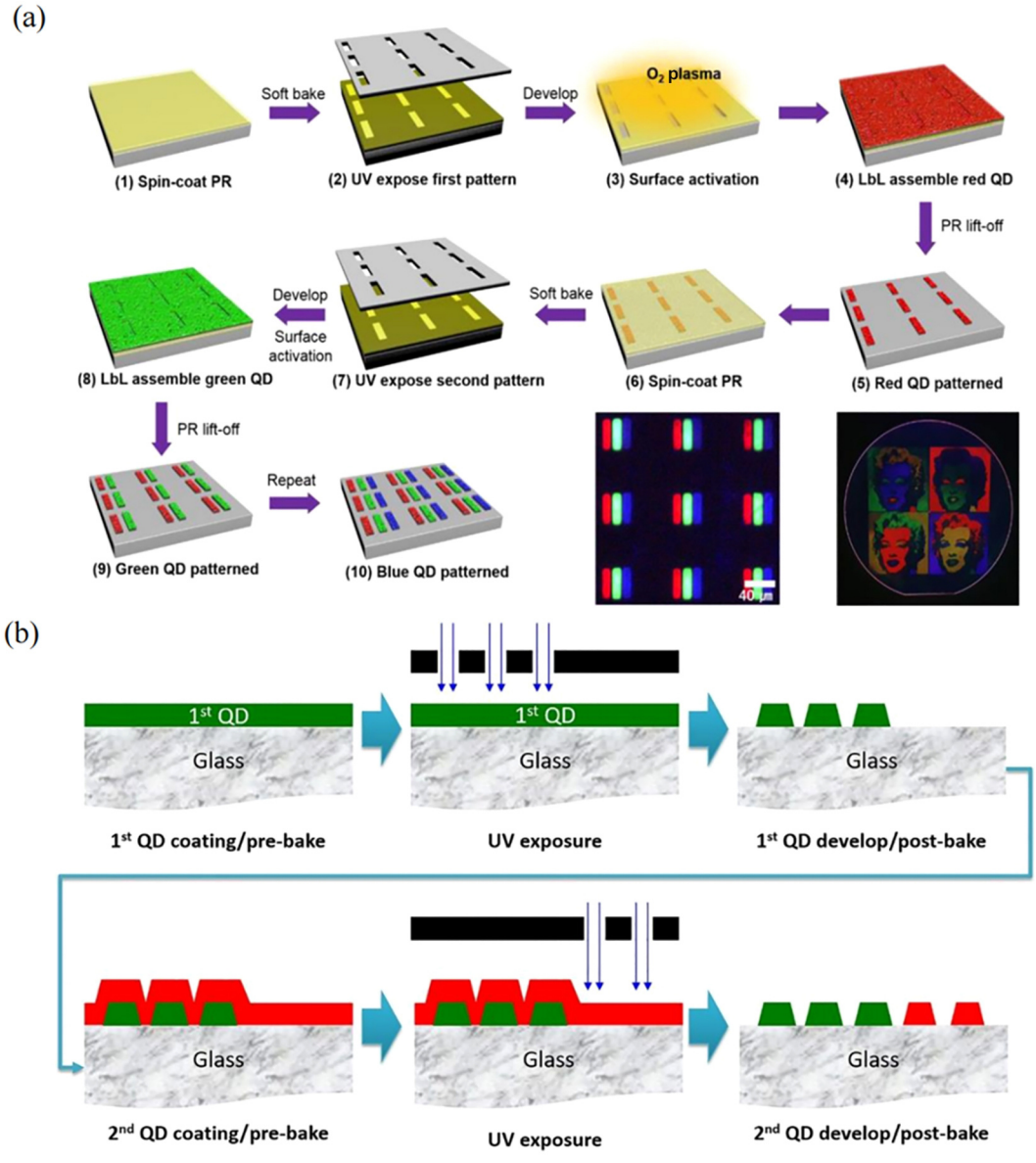

Figure 5 (a) Schematic diagram of patterning QDs layers using the photolithographic lift-off process. Reproduced with permission from Ref. [71], © American Chemical Society 2016. (b) Process of hybrid lithography of QDs and photoresist. Reproduced with permission from Ref. [76], © Society for Information Display 2019.

a QD solution with photoresist. Subsequently, this mixture was cured through a photolithography process and then developed using a tetramethylammonium hydroxide (TMAH) solution, as depicted in Fig. 5(b). In this process, PGMEA plays an important role as a solvent, making the mixing of the QD solution and photoresist efficient, as well as aiding in the coating and curing process of the photoresist. By precisely controlling the conditions of the photolithography process, the research team successfully prepared QD pattern arrays with a pixel size of 15 μm × 10 μm [76].

All of the aforementioned works accomplished QD patterning through physical lithography masks or photolithography methods by mixing QDs with photoresists. However, the compatibility of QDs with photoresist and organic polymer residues had an impact on the device performance [77]. Therefore, photolithography processes that introduce photosensitive ligands through ligand engineering have been developed to avoid these problems [73]. In 2020, Cho et al. utilized ligand engineering to create QD inks capped by long-chain organic surface ligands and a photoacid generator (PAG). Upon exposure to UV light, QDs of designated regions undergo a series of photochemical activation reactions with the PAG, leading to in situ ligand removal in the QD film (as shown in Fig. 6(a)), This leads to a significant change in the dissolution of the QDs, facilitating the formation of a QD pattern. Due to the high photosensitivity of PAG to UV (365 nm) or blue light (405 nm), high-resolution QD patterns with linewidths of 1.5 μm can be produced using small amounts of PAG (1 wt.%–3 wt.%) [78]. In 2020, Yang et al. constructed a QD with photosensitive ligands. This involved crosslinking and interlocking the ligands of neighboring QDs using cross-linking agents and photolithography, resulting in the curing of a QD pattern in a specified region, and the QDs in the non-patterned region were removed during the development process, as depicted in Fig. 6(b). Based on the light-driven cross-linking, they photopatterned CdSe-based core–shell QDs of different colors and prepared red, green, and blue QD patterns with sub-pixel sizes of 4 μm × 16 μm [79].

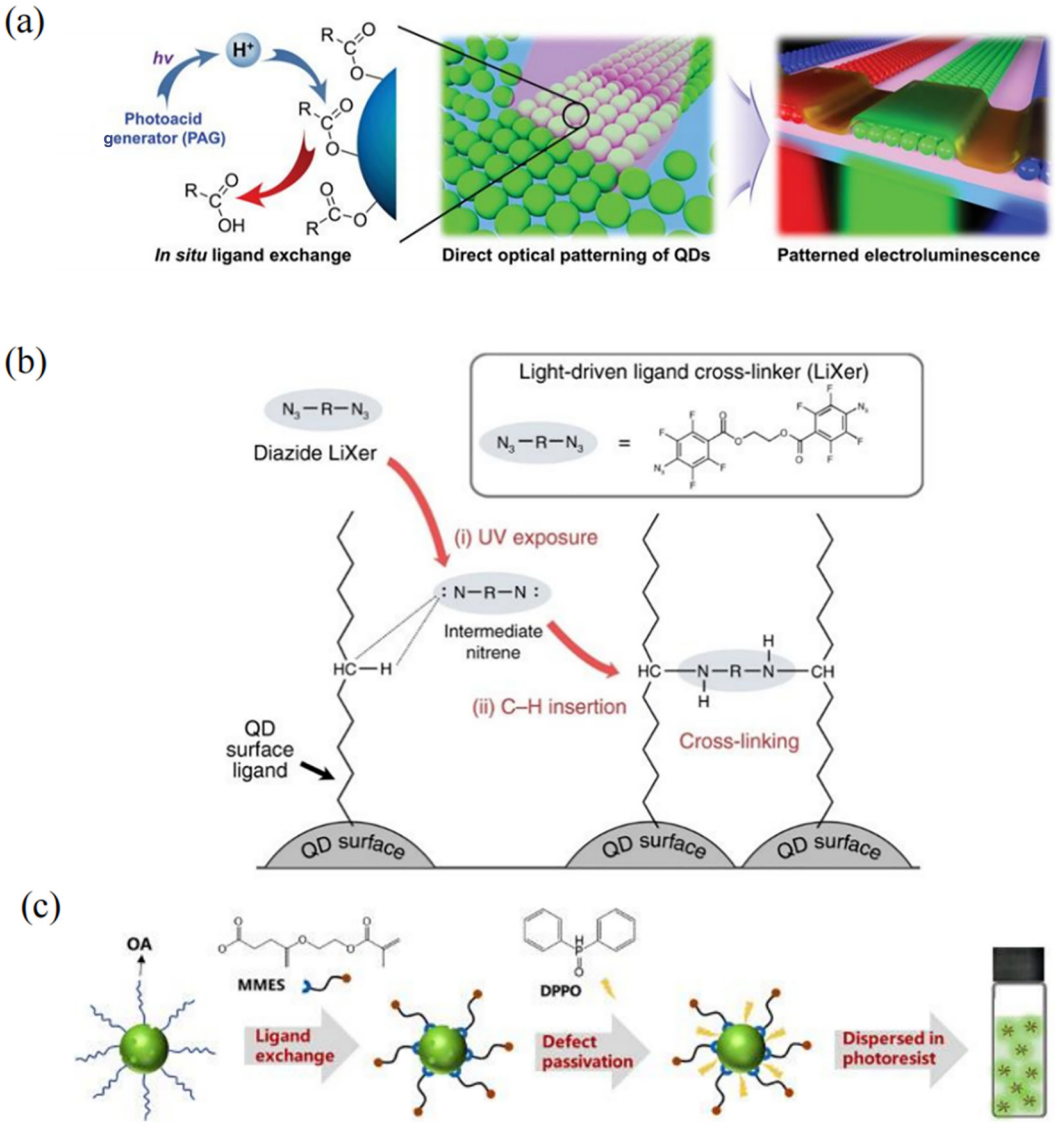

Figure 6 (a) Direct lithography using photosensitive ligands. Reproduced with permission from Ref. [78], © Wiley-VCH GmbH 2020. (b) Principle of photosensitive ligand-assisted lithography. Reproduced with permission from Ref. [79], © Yang, J. et al. 2020. (c) Patterning of QDs with high luminescence efficiency by ligand engineering and lithography process. Reproduced with permission from Ref. [80], © Wang, Y. K. et al. 2023.

The use of photosensitive ligand-assisted lithography and hybrid lithography for QDs and photoresists simplifies the process, but QDs have poor solubility in photoresists, necessitating ligand modification for compatibility [81–83]. Ligand modification and the introduction of photosensitive ligands usually reduce the fluorescence yield of QDs [84], impacting their stability, which remains a significant challenge in QD patterning. In 2023, our group developed a strategy to fabricate high-resolution QDCCs using a photolithographic process, which prepared highly luminescent and uniformly patterned QD layers through ligand engineering. The QDs were modified by replacing the native oleic acid ligand on the surface with succinic acid mono-2-(methacryloyloxy)ethyl succinate (MMES). Then a new ligand, diphenylphosphine oxide (DPPO), is introduced to repair the surface defects, as shown in Fig. 6(c). The passivation of DPPO is crucial for the luminescence performance of the QD film, which can significantly improve the photoluminescence quantum yield (PLQY) of QD films, achieving a value of 71.7% for green QD films [80].

In the case of perovskite QDs, since they are very sensitive to polar solvents, leading to a degradation of their performance [85], there is a need to coat the surface of perovskite QDs with a SiO_2 layer to improve their stability and make them compatible with conventional lithography processes. Zhang et al. proposed an *in situ* lithography technique for perovskite QDs based on photopolymerization catalyzed by lead bromide complexes. Perovskite QDs were successfully patterned by directly lithographing the precursor solution and synthesizing the PQDs in situ after exposure, avoiding the stripping process and the destruction of perovskite QDs by solvents or high-energy UV light. The pixel resolution can reach 2450 PPI and with high stability by controlling the polymerization and in situ fabrication conditions. What's more, patterns can be achieved on flexible substrates, which suggests a wider range of applications [86].

In summary, photolithography can achieve ultra-high-precision QD patterns and is highly compatible with existing semiconductor preparation processes and the possibility of large-scale preparation. However, hurdles exist, such as poor compatibility between QDs

and photoresists, modification of QD ligands results in decreased fluorescence yield of the QDs themselves, and the complex photolithographic lift-off process damages the QD layer. Furthermore, achieving high optical density (OD) values for QD films mixed with photoresist is challenging, which leads to insufficient absorption of blue light in the QDCC. Consequently, the addition of filter structures is required to eliminate unabsorbed blue light.

3.2.3 *Other QD patterning technologies*

In addition to inkjet printing and photolithography, researchers have proposed other ways to achieve QD patterning, which provide novel approaches for exploring the application of QDs in the realms of displays and optoelectronics.

Transfer technique. The transfer technique enables the transfer of a pre-prepared QD pattern from one substrate to another, as illustrated in Fig. 7(a). This technique typically transfers the QD pattern onto an elastic template or rubber film first with an appropriate transfer and then transfers it to the target substrate [87–89]. The transfer technique possesses advantages of high resolution, precision, and scalability, and is therefore widely used for preparing micro- and nanostructures as well as devices. Kim et al. prepared a full-color QD display with a sub-pixel size of 46 μm × 96 μm using transfer printing technology. They first spin-coated a layer of QDs on a donor substrate, which was subsequently picked up onto a letterpress elastic polydimethylsiloxane impression using surface energy and van der Waals forces. The picked-up QDs were then transferred to the acceptor substrate utilizing weak interactions between the alkane groups on its surface and the aliphatic ligands on the QD surface, thereby forming a large-area patterned, pixelated, and full-color QD layer through the repetition of the transfer printing process [60]. Currently, transfer printing technology can achieve high-speed and large-scale high-resolution QD patterning [90], but the deformation and loss of the stamp structure during multiple transfers reduce the precision and reliability of its production process.

Microporous filling. Microporous filling is a method that fills QD solution into micron-scale pore structures, as depicted in Fig. 7(b). Micropores can be prepared from templates or formed by the self-assembly of nanoparticles. The directional self-assembly and alignment of QDs within the micropores can be achieved by controlling parameters such as the wettability and surface tension of the solution, leading to the formation of patterned QD structures. In 2023, Sun et al. prepared a pixel-size 6 μm circular green QD color conversion array using the micropore filling fabrication. The desired pixel patterns were fabricated on a glass substrate via the standard photoresist process on SU-8 photoresist to form an SU-8 micropore mold. Subsequently, a certain amount of QD gel was dripped onto the SU8 micropore mold, and the QDs were applied by scraping to fill the micropores and remove the excess QDs on the surface. After curing, a pixelated QD pattern was formed, and the residual QDs outside the pores were removed by a polishing process [91].

Electrophoretic deposition. In electrophoretic deposition, the directional deposition of QDs on a conductive substrate is driven by an electric field. When subjected to an appropriate electric field, QDs can form patterns on the surface of the substrate, as depicted in Fig. 7(c), which is simple, fast, low-cost, and can prepare QD patterns over large areas. In 2021, Zhao et al. used electrophoretic deposition to prepare QD arrays with pixel dimensions of 14.6 μm × 30.5 μm. The colloidal CdSe/ZnS core/shell QDs were capped with polyethylene glycol (PEG)–COOH in PGMEA to make the carboxyl groups on their ligands negatively charged after ionization. Subsequently, the QDs were deposited onto electrodes of the opposite electrical properties through the action of an electric field to form a patterned QDCC [92]. While electrophoretic deposition

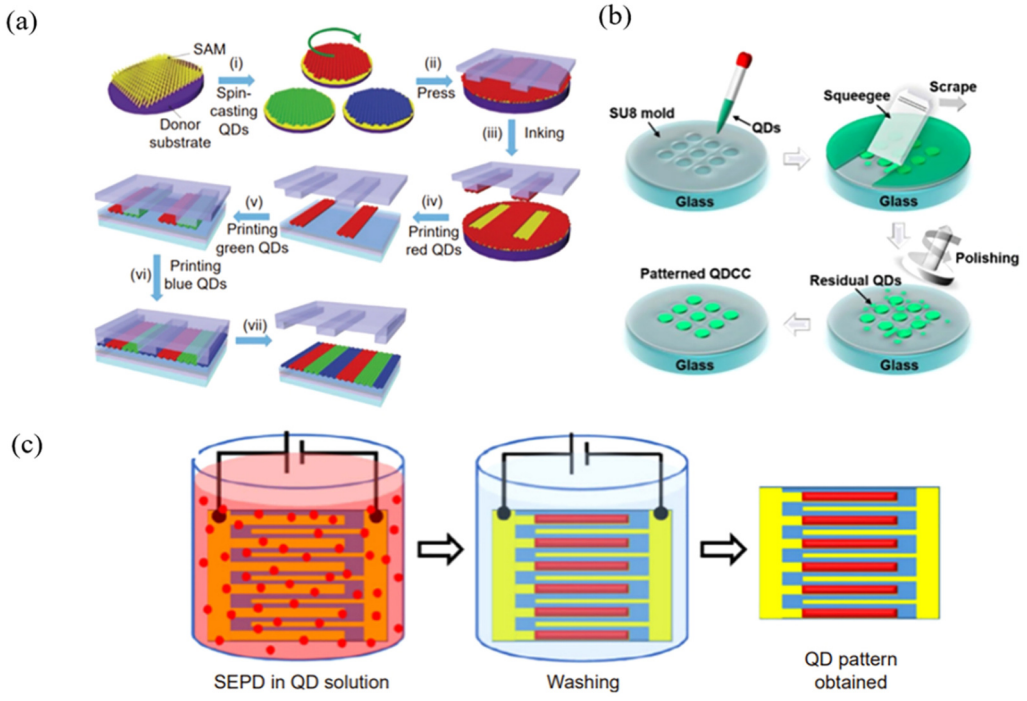

Figure 7 (a) Flow of patterning QDs using the transfer technique. Reproduced with permission from Ref. [60], © Springer Nature Limited 2011. (b) Flow of preparing QD patterns using microporous filling method. Reproduced with permission from Ref. [91], © The Royal Society of Chemistry 2022. (c) Flow of depositing QDs on a substrate by electrophoretic deposition. Reproduced with permission from Ref. [92], © Zhao, J. Y. et al. 2021.

offers a rapid means of achieving large-area QD deposition, it imposes higher requirements on the preparation process of patterned microelectrodes.

Three-dimensional (3D) printing. QD patterning can also be achieved through 3D printing [93]. Kong et al. demonstrated the potential of 3D printing in QDs patterning by preparing QDs-based light-emitting diodes with pure and tunable color-emission properties, demonstrating the potential of 3D printing in QDs patterning in the context of integrating different materials in QLEDs [94]. In 2022, Zhao et al. proposed a laser direct writing technique for photoexcitation-induced chemical bonding, enabling laser 3D assembly of QDs. This process is capable of 3D printing arbitrary QD structures at resolutions beyond the diffraction limit, thus establishing it as a promising approach for developing 3D QLEDs [95].

Laser direct writing. Xu et al. used a continuous wave laser to directly induce the *in situ* synthesis of perovskite in a poly(methyl methacrylate) matrix. By adjusting the type and content of halogen ions in the precursor solution, tunable perovskite with PL spectrum in the range of 475 to 667 nm is achieved. Under the combined influence of the photonic effect and thermal quenching in perovskite, they achieved ultrahigh-precision patterning, with a minimum linewidth of 750 nm and a maximum pixel density of 5684 PPI, and the patterning film can be utilized for flexible displays [96].

In summary, the study shows that diverse QD patterning techniques, such as inkjet printing, photolithography, transfer printing, 3D printing, and Laser direct writing, have their own advantages and shortcomings, and they are summarized in Table 2. Efforts are being made by researchers to further explore and enhance these methods for achieving more efficient and precise QD patterning. These innovative technological solutions provide expanded possibilities for the application of QDs in display, optoelectronics, and micro-LEDs, thereby fostering the development and progress of related fields.

From a material perspective, QDs used as color converters can be classified into Cd-based QDs, [80] perovskite QDs [97], and heavy-metal-free QDs [98–100]. In terms of forms of QD color converters, they can be classified into mainly three types: (i) encapsulating QDs within microspheres to improve stability [49, 101]; (ii) QD-dominated films that are achieved by crosslinking the ligands [78, 79]. (iii) QDs in a polymer matrix enabled by photolithography or inkjet printing techniques [15, 16, 75, 76].

3.3 QD micro-LED display configuration

From a practical application perspective, QDs are commonly used in micro-LEDs as a color converter on blue/UV LEDs or combing them with nanostructures to achieve full-color through blue/UV excitation of color conversion materials. Filter structures can be integrated into the device to effectively absorb blue light. DBRs are several pairs of semiconductor or dielectric materials grown in a staggered fashion to achieve high reflectivity within a specific optical band. The DBR structure can be incorporated on top of the QDCC to enhance the reflection of blue light, reflecting any blue light that is not sufficiently absorbed by QDs. This process enhances the absorption of blue light by QDs, thus improving luminous efficiency and color purity. Han et al. used aerosol inkjet printing to spray QDs on UV LEDs and encapsulated a DBR on the top to reflect the UV light [15]. The highest reflectivity of DBR is at 400 nm, to transmit red, green, and blue light, enhancing UV light utilization and increasing color purity. The addition of DBR resulted in a 194% increase in visible light OD values for blue, and 173% and 183% increases for green and red, respectively. The device is schematically depicted in Fig. 8(a). Chen et al. simultaneously deposited HBR at the bottom, in addition to using DBR at the top, to further reflect downward-transmitted red and green light [17]. The use of HBR and DBR increased the OD value of red and green light in micro-LEDs by 27%. Additionally, black photoresist was used to wrap every pixel point to prevent color crosstalk, and this approach improved the micro-LED contrast ratio from 11 to 22. Chu et al. deposited a blue-light absorbing layer on the DBR of the above structure, resulting in an improvement of red-green color purity to 90.9% and 90.3% [102], as illustrated in Fig. 8(b).

In addition to the use of DBR, blue light absorption and color purity can be improved in other ways. Hsiang et al. designed a CLC polymer film, employing a patterned photomask to create two kinds of textures on the CLC film, focal conic texture (FC-CLC) and planar texture (P-CLC) during the UV curing process [19]. The P-CLC, acting as a DBR, is on the red and green sub-pixels to efficiently reflect leaked blue light. While the FC-CLC is on the blue sub-pixels, serving as a scattering medium to replace traditional scattering particles, reducing the mismatched angular radiation patterns of RGB sub-pixels and the color shift. The device structure, as depicted in Fig. 8(c), involved depositing a QDCC on the blue micro-LED, followed by the application of the CLC film and a color filter to further enhance color purity. The design can improve the CCE of the display system by about 143%. Moreover, the polymer film design offered cost-efficiency and simplicity in manufacturing compared to traditional DBR techniques.

The QDCCs can also be used with nanostructures. This approach reduces the energy loss and improves the CCE and

Table 2 Comparison of QD patterning technologies

Patterning technology	Advantages	Disadvantages
Inkjet printing	Low-cost, non-contact, small material loss	Coffee-ring effect\low production efficiency of inkjet printing equipment
Photolithography	High precision, compatible with semiconductor processes	High-cost, residues affect device performance
Transfer technique	High precision, without organic additives	The seal structure deformation\contact wear
Microporous filling	Low-cost, high processing efficiency	Relatively low precision\low device performance
Electrophoretic deposition	Rapid fabrication rate, simplified manufacturing process	The fabrication process of microelectrodes is complex
3D printing	High degree of flexibility, low material consumption	High-cost\low processing efficiency
Laser direct writing	High precision, applicable to flexible displays	High-cost\complex fabrication process

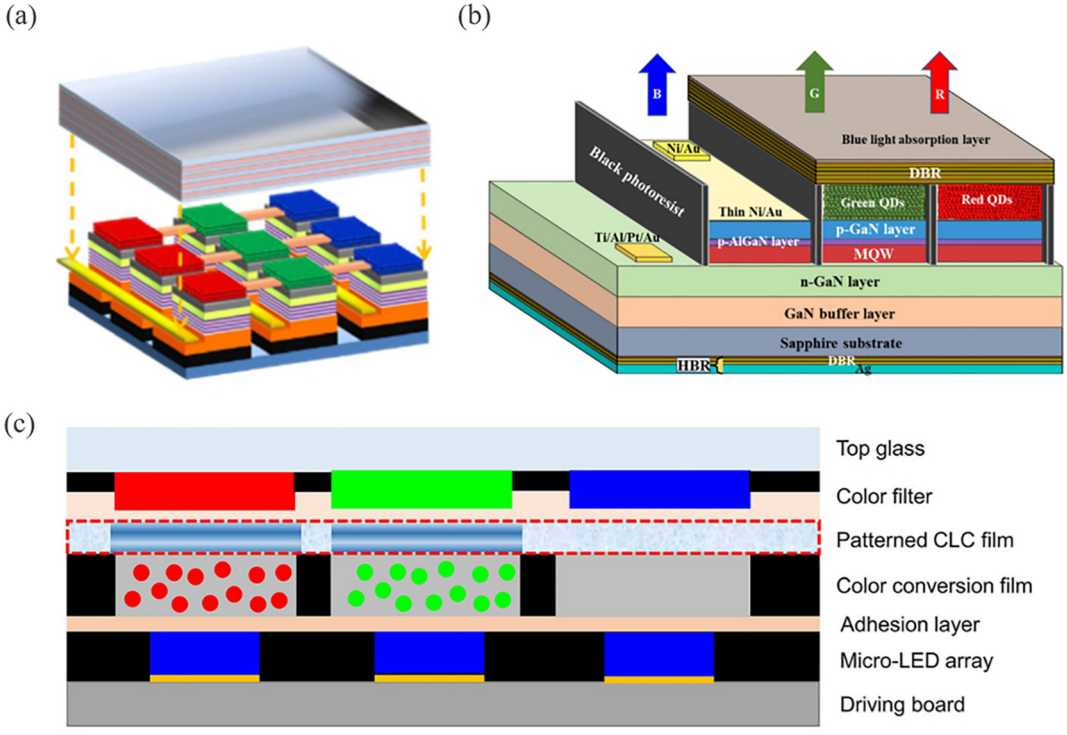

Figure 8 (a) Device structure of QD-based micro-LED display. Reproduced with permission from Ref. [15], © Optical Society of America 2015. (b) Schematic structure of monolithic full-color micro-LED using QDCCs. Reproduced with permission from Ref. [102], © Chu, S. Y. et al., Licensee MDPI, Basel, Switzerland 2020. (c) Schematic structure of QD-micro-LED device with CLC polymer film. Reproduced with permission from Ref. [20], © Society for Information Display 2021.

quantum yield by non-radiative energy transfer (NRET), mainly through the close contact between the donor and the acceptor [18]. Krishnan et al, designed a nanohole structure (Fig. 9(a)) and fabricated a hybrid 12-fold photonic quasi-crystal (PQC) by nanolithography as well as plasma etching, where the PQC structure penetrated the MQW active region to create a cylindrical array of holes with a radius of 480 nm and a lattice spacing of 750 nm [103]. Since the QDs are very close to the active region, the PLQY can be well enhanced. Subsequently, QDs with emission wavelengths of 535, 585, and 630 nm were spin-coated into the nanohole arrays, and the devices were engineered to emit white light by adjusting the mixing ratio of the QDs. The effective quantum yield (EQY) of monochromatic and mixed-color white light was investigated, revealing an EQY of up to 123% for monochromatic light, while for mixed-color light, the EQY decreased compared to monochromatic light due to the existence of radiative and non-radiative energy transfer between the different colors, reaching up to 110%, a more than 30% improvement compared to previously reported values. Song et al. investigated the EQY of white light in a nanohole array of nanoporous GaN (NP-GaN) embedded QDs and achieved full color [104]. This structure significantly increased light scattering, and thus dramatically improved the absorption of blue light by the QDs within NP-GaN, as depicted in Fig. 9(b). A monolithic full-color micro-LED was fabricated on the same epitaxial wafer, with each micro-LED matrix measuring approximately 35 μm × 35 μm. The light conversion efficiencies of the NPQDs were up to 94% for the red NPQDs and about 63% for the green ones. Yang's group, discovered that when QDs are inserted into a GaN porous structure (PS), the Förster resonance energy transfer (FRET) efficiency is enhanced, indicating that the nanoscale-cavity effect can improve FRET efficiency [105]. They designed a device structure in which QDs are integrated into a GaN PS, leveraging surface plasmon (SP) coupling effects to achieve a favorable nanoscale-cavity effect, and deposited surface Ag nanoparticles to induced SP coupling, significantly enhancing the FRET efficiency of the QWs to QDs [106].

Chen et al. designed micro-LEDs with NR structures, as illustrated in Fig. 9(c) [18]. In this design, each pixel measured 3 μm × 10 μm, and every colored pixel comprised a green pixel and two NR array pixels. The width of the nanoring wall was adjusted through strain-induced engineering, with an outer diameter of 700 nm and an inner diameter of 900 nm of the NR, and the color of the NR-micro-LED was modified from green to blue. Subsequently, the red pixel display was achieved by applying CdSe/ZnS red QDs onto the blue LEDs, resulting in a linewidth of 2 μm, which is a significant improvement in accuracy compared to the previous linewidth range of 30–40 μm. Meanwhile, an atomic layer deposition passivation layer was deposited on the side wall to enhance the display lifespan and performance stability, leading to a 143.7% increase in luminous intensity. In addition, a layer of DBR was applied to the red pixel to further enhance the efficiency of red-light emission, realizing a broad color gamut for the QD-NR-micro-LEDs.

4 Main challenges

Despite the variety of patterning techniques and device configurations available for QDs in micro-LED displays, there are still several challenges that must be addressed, including the enhancement of blue light absorption, the improvement of device stability device stability, and the development of environment-friendly QD materials.

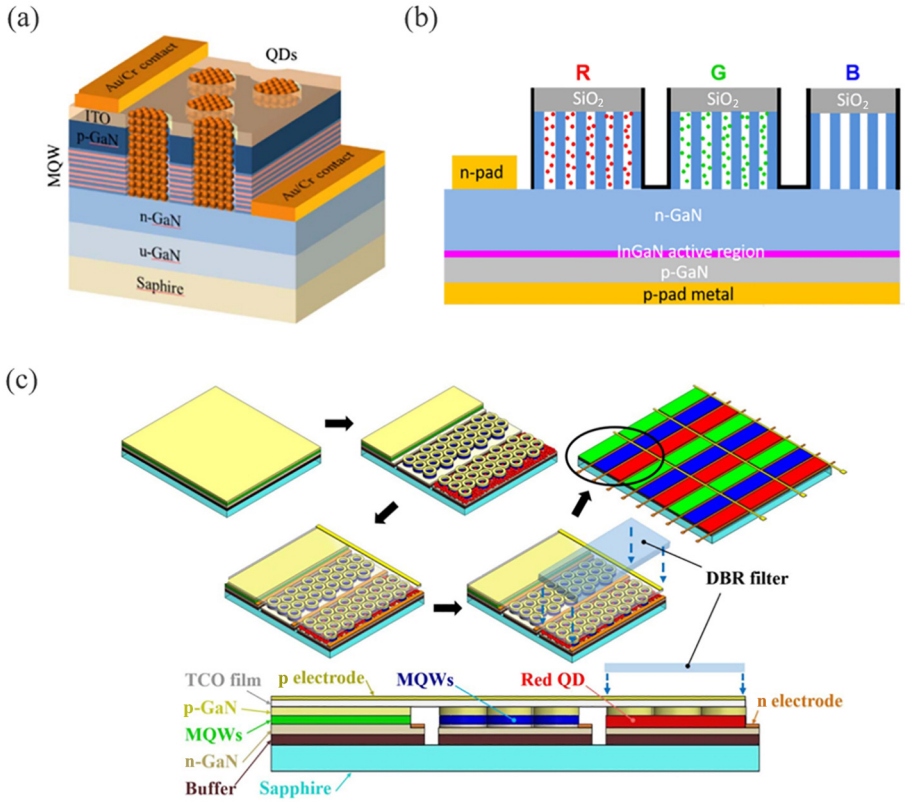

Figure 9 (a) Schematic diagram of nanohole QD-micro-LED with PQC structure. Reproduced with permission from Ref. [103], © Optical Society of America 2016. (b) Schematic cross-sectional view of monolithic full-color NPQD-micro-LED. Reproduced with permission from Ref. [104], © American Chemical Society 2021. (c) Schematic diagram of NR-QD-micro-LED fabrication process and structure. Reproduced with permission from Ref. [18], © Chinese Laser Press 2019.

4.1 Blue light absorption

QD-micro-LEDs operate by converting received short-wavelength blue light into long-wavelength red and green light. Incomplete absorption of blue light will result in the leakage of blue light, thereby impacting color purity and the final display effect. According to the Beer–Lambert law analysis, achieving full absorption of blue light typically requires an OD value of the QDCC over 3, and the QD film thickness needs to reach approximately 10 μm [76]. During the photolithography process, to increase the OD value of the QDCC, the concentration of QDs in the photoresist should be increased, which imposes higher demands on the solubility of both QDs and photoresist. However, excessive QD concentration in the photoresist will affect the photosensitive properties of the photoresist, consequently affecting photolithography process parameters. In addition to increasing the concentration of quantum dots, the absorption effect of blue light can also be enhanced by increasing the thickness of the color converter. However, the achievable thickness of the photoresist is limited by the spin coating process, and the uniformity will also be affected as the thickness increases. Furthermore, an excessively thick film can also aggravate the self-absorption effect of quantum dots.

The optical properties and blue light absorption can also be enhanced by adding scattering particles such as SiO_2, TiO_2, and other nanoparticles. Adding scattering particles uses the scattering effect of the material on light, altering the optical path of blue light within the QDCC and extending the optical range, thus increasing the likelihood of exciting the QD material and improving conversion efficiency. In 2020, Theobald et al. incorporated nanoparticles into a QD layer based on a light-scattering design. This design acted as a selective reflector to extract the conversion light while boosting the absorption of incident excitation light by more than fourfold [107]. These schemes offer valuable insights for the development of QD-micro-LEDs. They provide methods to enhance blue light absorption by increasing the thickness of the QDCC and designing the optical structure to meet practical applications. However, the addition of an excessive amount of scattering particles is prone to causing agglomeration. When particle concentration becomes too high, it negatively impacts the diffraction effect, resulting in a loss of light output [108]. Additionally, the addition of scattering particles might also reduce the resolution that can be achieved by photolithography. Therefore, simply increasing the concentration of scattering particles is not recommended.

4.2 Stability

Considering the advantages of the high color gamut and resolution offered by QD-micro-LEDs, they are expected to be applied in near-eye display scenarios such as VR & AR is feasible [109]. QDs used in micro-LED device fabrication must endure temperatures over 100 °C and intense blue light exposure of thousands of nits, indicating a harsh working environment. The optical display system of AR devices typically comprises a miniature display and optical waveguide elements, and the conversion efficiency of the optical waveguide is < 10%. Consequently, the demand for micro-LED display brightness is substantially high (~ 100,000 nits), and the QDCC must withstand very high blue radiant power (~ 6 W/cm^2) [110]. QDs are sensitive to environmental conditions. Under

illumination, a brief exposure to water and oxygen will lead to photoactivation of the QDs. Over time, however, the QDs will be quenched due to corrosion caused by water and oxygen [111–113]. Although some QDs tend to exhibit better stability in pure water or pure oxygen environments due to the difference in the core-shell structures, they are still difficult to maintain stability when simultaneously exposed to both water and oxygen [114, 115]. Additionally, high-temperature environments can lead to irreversible defects in the QDs and negatively impact their luminescent efficiency [116–118]. In recent years, the stability of QDs has been significantly improved through strategies such as dual-ligand synergistic effects [119], lattice stress regulation [120], and packaging of QDs [49, 101]. For example, in 2024, Wang et al. employed a dual-ligand strategy to create long-range ordered, dense, and defect-free perovskite QD films, greatly boosting device performance and stability [119]. In 2022, He et al. wrapped $CsPbBr_3$ QDs inside the SiO_2 spheres by using the selective sintering characteristics of K_2CO_3 inside SiO_2 spheres. Isolating the QDs from oxygen and moisture improves the stability and lifetime of the QDs. In stability testing, up to 94% of the initial emission intensity was preserved after 1000 h of continuous illumination from a blue LED (450 nm, 3500 cd/m^2). Additionally, encapsulation within SiO_2 spheres improves the dispersion of QDs, facilitating uniform dispersion in liquids or solids without causing cross-linking and aggregation of the particles. Consequently, this method is also suitable for lithography processes mixed with photoresists [49]. In 2025, Gong et al. synthesized QD@dMS@PMAO@SiO_2 microspheres via a wet chemical process. These microspheres not only preserved the optical properties of QDs but also exhibited high stability against environmental factors like water, oxygen, blue light, and heat without water-oxygen barrier layers [101]. Furthermore, functional nanomaterials with higher surface energy (calcium nanoparticles, barium nanoparticles, etc.) can be employed as desiccants. Due to their smaller size, nanoparticles have higher surface energy and are more likely to combine and react with oxygen and water. Consequently, they absorb oxygen and water within the functional layer of the QDs, avoiding potential damage and augmenting device stability. Moreover, the oxides generated from these functional nanomaterials can serve as light-scattering particles, thereby enhancing light scattering and further improving the optical characteristics of the QDs [121].

4.3 Environment-friendly

Current research on QD-micro-LEDs is mainly based on Cd-based QDs or Pb-containing perovskite QDs, which possess high toxicity. Despite the superior photoelectric performance and chemical stability of Cd-based core–shell structure QDs, the presence of the heavy metal Cd raises toxicity concerns. Currently, the toxicity of CdSe QDs can be mitigated through surface modification, shell layer coating, functionalization, etc. However, it is still necessary to develop Cd-free QD materials exhibiting high PLQY, narrow emission width, and well stability to fulfill the requirements of practical applications for QD-micro-LEDs. ZnSe, InP, and $CuInSe_{2-x}S_x$ are all green and environment-friendly QDs suitable for display applications. However, ZnSe QDs possess a large bandgap and emit violet light, need to be doped with Te, etc. to expand their emission to a longer wavelength, which will inevitably introduce defects and reduce luminescence efficiency [122, 123]. $CuInSe_{2-x}S_x$ has a broader emission spectrum and low color purity. InP, on the other hand, shows promise as a Cd-free alternative due to its visible-range luminescence and narrower peak width [124]. Nevertheless, InP QDs are prone to surface defects, which lead to non-radiative recombination, affect the luminescence efficiency, and need to be coated with ZnSe or ZnS shells to improve their PLQY [125]. Practical applications still face technological and material challenges that must be addressed to enhance optical properties, stability, and control over the preparation process, aligning better with the requirements of display technologies.

5 Conclusion and perspective

With the increasing demands for improved display performance, micro-LED, as a new generation of display technology, has attracted much attention for its wide color gamut, extended lifespan, and wide range of applications. QDs, with their advantages of small size, narrow full width at half maximum, high color purity, etc., can be used as the main medium to achieve full-color micro-displays.

Although many studies have investigated the use of QDs in micro-LED technology, there are still many challenges in applying QDs to micro-LED displays. One significant obstacle is the complexity of patterning technology, while the use of high-precision and compatibility with semiconductor processes photolithography is preferred. To enhance the absorption of blue light, incorporating scattering particles and adding the DBR structure can effectively improve the excitation of QDs for better CCE. Despite relatively minimal concerns regarding the stability of QDs, the application of micro-LEDs inevitably has to face the impact of strong blue light and high temperatures, to ensure the stability of QDs in the strict environment presents a major challenge.

In short, from QD patterning technology to conversion efficiency to luminous stability and other aspects, there is still a long way to go to realize the commercial application of quantum dots in micro-LED displays. Owning to the unresolved technical complexities, micro-LEDs cannot replace LCD and OLED displays in the short term, but they exhibit significant advantages within the realm of VR/AR applications. Moreover, the combination of QD and micro-LED will be further developed to achieve higher CCE and light output efficiency, expediting to prompt widespread adoption of micro-LED technology.

Data availability

All data needed to support the conclusions in the paper are presented in the manuscript. Additional data related to this paper may be requested from the corresponding author upon request.

Acknowledgements

This work was supported by the National Key R&D Program of China (No. 2021YFA0715502) and the National Natural Science Foundation of China (No. 62475084).

Declaration of competing interest

All the contributing authors report no conflict of interests in this work.

Author contribution statement

Y. Q. Z.: Literature research, data collection, manuscript writing,

figure preparation. W. Z. Q.: Literature research, data collection, manuscript writing, figure preparation. R. L.: Discussion and revision. X. Z.: Discussion and revision. F. Q. M.: Discussion and revision. J. J. L.: Discussion and revision. L. Y. L. (corresponding author): Review and editing, project management. D. L. Z. (corresponding author): Review and editing, project management. J. B. Z. (corresponding author): Topic suggestion, project management, review and editing. All the authors have approved the final manuscript.

Use of AI statement

During the preparation of this work, the authors used ChatGPT & Deepseek, in order to check for grammatical errors and improve the readability and fluency. After using this tool, the authors reviewed and edited the content as needed and take full responsibility for the content of the publication.

References

[1] Ding, K.; Avrutin, V.; Izyumskaya, N.; Özgür, Ü.; Morkoç, H. Micro-LEDs, a manufacturability perspective. *Appl. Sci.* **2019**, *9*, 1206.

[2] Ryu, J. E.; Park, S.; Park, Y.; Ryu, S. W.; Hwang K.; Jang, H. W. Technological breakthroughs in chip fabrication, transfer, and color conversion for high-performance micro-LED displays. *Adv. Mater.* **2023**, *35*, 2204947.

[3] Ma, T.; Chen, J.; Chen, Z. Y.; Liang, L. M.; Hu, J. N.; Shen, W. L.; Li, Z. H.; Zeng, H. B. Progress in color conversion technology for micro-LED. *Adv. Mater. Technol.* **2023**, *8*, 2200632.

[4] Chen, Z.; Yan, S. K.; Danesh, C. MicroLED technologies and applications: Characteristics, fabrication, progress, and challenges. *J. Phys. D: Appl. Phys.* **2021**, *54*, 123001.

[5] Miao, W. C.; Hsiao, F. H.; Sheng, Y. J.; Lee, T. Y.; Hong, Y. H.; Tsai, C. W.; Chen, H. L.; Liu, Z. J.; Lin, C. L.; Chung, R. J. et al. Microdisplays: Mini-LED, micro-OLED, and micro-LED. *Adv. Opt. Mater.* **2024**, *12*, 2300112.

[6] Xiong, J. H.; Hsiang, E. L.; He, Z. Q.; Zhan, T.; Wu, S. T. Augmented reality and virtual reality displays: Emerging technologies and future perspectives. *Light: Sci. Appl.* **2021**, *10*, 216.

[7] Zhou, J.; Yan, J. J.; Liu, Z. Q.; Jiang, Y.; Huang, K.; Bao, K.; Li, J. C.; Zhou, D. Y. The current bottleneck and technical progress of micro LED. *Optoelectron. Technol.* **2023**, *43*, 91–113.

[8] Seymour, J. P.; Wu, F.; Wise, K. D.; Yoon, E. State-of-the-art MEMS and microsystem tools for brain research. *Microsyst. Nanoeng.* **2017**, *3*, 16066.

[9] McAlinden, N.; Massoubre, D.; Richardson, E.; Gu, E. D.; Sakata, S.; Dawson, M. D.; Mathieson, K. Thermal and optical characterization of micro-LED probes for *in vivo* optogenetic neural stimulation. *Opt. Lett.* **2013**, *38*, 992–994.

[10] Yeo, K. S.; Ng, W. X; Soh, M, Y.; Teo, T. H. Micro-LED arrays for display and communication: Device structure and driver architecture. In *Proceedings of the IEEE 12th International Conference on ASIC*, Guiyang, China, 2017, pp 993–996.

[11] Islim, M. S.; Ferreira, R. X.; He, X. Y.; Xie, E. Y.; Videv, S.; Viola, S.; Watson, S.; Bamiedakis, N.; Penty, R. V.; White, I. H. et al. Towards 10 Gb/s orthogonal frequency division multiplexing-based visible light communication using a GaN violet micro-LED. *Photonics Res.* **2017**, *5*, A35–A43.

[12] Jin, S. X.; Li, J.; Li, J. Z.; Lin J. Y.; Jiang, H. X. GaN microdisk light emitting diodes. *Appl. Phys. Lett.* **2000**, *76*, 631–633.

[13] Liu, Z. J.; Wong, K. M.; Chong, W. C.; Lau, K. M. P-34: Active matrix programmable monolithic light emitting diodes on silicon (LEDoS) displays. *SID Symp. Dig. Tech. Pap.* **2011**, *42*, 1215–1218.

[14] Liu, Z. J.; Chong, W. C.; Wong, K. M.; Tam, K. H.; Lau, K. M. A novel BLU-free full-color LED projector using LED on silicon micro-displays. *IEEE Photonics Technol. Lett.* **2013**, *25*, 2267–2270.

[15] Han, H. V.; Lin, H. Y.; Lin, C. C.; Chong, W. C.; Li, J. R.; Chen, K. J.; Yu, P. C.; Chen, T. M.; Chen, H. M.; Lau, K. M. et al. Resonant-enhanced full-color emission of quantum-dot-based micro LED display technology. *Opt. Express* **2015**, *23*, 32504–32515.

[16] Lin, H. Y.; Sher, C. W.; Hsieh, D. H.; Chen, X. Y.; Chen, H. M. P.; Chen, T. M.; Lau, K. M.; Chen, C. H.; Lin, C. C.; Kuo, H. C. Optical cross-talk reduction in a quantum-dot-based full-color micro-light-emitting-diode display by a lithographic-fabricated photoresist mold. *Photonics Res.* **2017**, *5*, 411–416.

[17] Chen, G. S.; Wei, B. Y.; Lee, C. T.; Lee, H. Y. Monolithic red/green/blue micro-LEDs with HBR and DBR structures. *IEEE Photonics Technol. Lett.* **2018**, *30*, 262–265.

[18] Chen, S. W. H.; Shen, C. C.; Wu, T. Z.; Liao, Z. Y.; Chen, L. F.; Zhou, J. R.; Lee, C. F.; Lin, C. H.; Lin, C. C.; Sher, C. W. et al. Full-color monolithic hybrid quantum dot nanoring micro light-emitting diodes with improved efficiency using atomic layer deposition and nonradiative resonant energy transfer. *Photonics Res.* **2019**, *7*, 416–422.

[19] Hsiang, E. L.; Li, Y. N. Q.; He, Z. Q.; Zhan, T.; Zhang, C. C.; Lan, Y. F.; Dong, Y. J.; Wu, S. T. Enhancing the efficiency of color conversion micro-LED display with a patterned cholesteric liquid crystal polymer film. *Nanomaterials* **2020**, *10*, 2430.

[20] Hsiang, E. L.; Li, Y. N. Q.; He, Z. Q.; Zhan, T.; Zhang, C. C.; Lan, Y. F.; Dong, Y. J.; Wu, S. T. 62-4: Doubling the optical efficiency of color-converted micro-light-emitting diode displays with a patterned cholesteric liquid crystal polymer film. *J. Soc. Inf. Disp.* **2021**, *29*, 288–297.

[21] Liu, Z. J.; Wong, K. M.; Keung, C. W.; Tang C. W.; Lau, K. M. Monolithic LED microdisplay on active matrix substrate using flip-chip technology. *IEEE J. Sel. Top. Quant. Electron.* **2009**, *15*, 1298–1302.

[22] Olivier, F.; Tirano, S.; Dupré, L.; Aventurier, B.; Largeron, C.; Templier, F. Influence of size-reduction on the performances of GaN-based micro-LEDs for display application. *J. Lumin.* **2017**, *191*, 112–116.

[23] Olivier, F.; Daami, A.; Licitra, C.; Templier, F. Shockley-Read-Hall and Auger non-radiative recombination in GaN based LEDs: A size effect study. *Appl. Phys. Lett.* **2017**, *111*, 022104.

[24] Konoplev, S. S.; Bulashevich, K. A.; Karpov, S. Y. From large-size to micro-LEDs: Scaling trends revealed by modeling. *Phys. Status Solidi (a)* **2018**, *215*, 1700508.

[25] Kim, D. H.; Park, Y. S.; Kang, D.; Kim, K. K.; Seong T. Y.; Amano, H. Combined effects of V pits and chip size on the electrical and optical properties of green InGaN-based light-emitting diodes. *J. Alloy. Compd.* **2019**, *796*, 146–152.

[26] David, A.; Young, N. G.; Hurni, C. A.; Craven, M. D. Quantum efficiency of III-nitride emitters: Evidence for defect-assisted nonradiative recombination and its effect on the green gap. *Phys. Rev. Appl.* **2019**, *11*, 031001.

[27] Zhang, S. N.; Zhang, J. L.; Gao, J. D.; Wang, X. L.; Zheng, C. D.; Zhang, M.; Wu, X. M.; Xu, L. Q.; Ding, J.; Quan, Z. J. et al. Efficient emission of InGaN-based light-emitting diodes: Toward orange and red. *Photonics Res.* **2020**, *8*, 1671–1675.

[28] Horng, R. H.; Ye, C. X.; Chen, P. W.; Iida, D.; Ohkawa, K.; Wu Y. R.; Wuu, D. S. Study on the effect of size on InGaN red micro-LEDs. *Sci. Rep.* **2022**, *12*, 1324.

[29] Oh, J. T.; Lee, S. Y.; Moon, Y. T.; Moon, J. H.; Park, S.; Hong, K. Y.; Song, K. Y.; Oh, C.; Shim, J. I.; Jeong, H. H. et al. Light output performance of red AlGaInP-based light emitting diodes with different chip geometries and structures. *Opt. Express* **2018**, *26*, 11194–11200.

[30] Wu, Y. F.; Ma, J. S.; Su, P.; Zhang, L. J.; Xia, B. Z. Full-color realization of micro-LED displays. *Nanomaterials* **2020**, *10*, 2482.

[31] Zhang, S. H.; Zheng, H.; Zhou, L.; Li, H. D.; Chen, Y. R.; Wei, C.

C.; Wu, T.; Lv, W.; Zhang, G.; Zhang, S. Q. et al. Research progress of micro-LED display technology. *Crystals* **2023**, *13*, 1001.

[32] Meitl, M. A.; Zhu, Z. T.; Kumar, V.; Lee, K. J.; Feng, X.; Huang, Y. Y.; Adesida, I.; Nuzzo, R. G.; Rogers, J. A. Transfer printing by kinetic control of adhesion to an elastomeric stamp. *Nat. Mater.* **2006**, *5*, 33–38.

[33] Feng, L.; Meitl, M. A.; Bowen, A. M.; Huang, Y. G.; Nuzzo, R. G.; Rogers, J. A. Competing fracture in kinetically controlled transfer printing. *Langmuir* **2007**, *23*, 12555–12560.

[34] Wu, M. H.; Fang, Y. H.; Chao, C. H. Electric-programmable magnetic module and picking-Up and placement process for electronix devices. U.S. Patent 9,607,907, June 16, 2016.

[35] Bibl, A.; Higginson, J. A.; Law, H. F. S.; Hu, H. H. Micro device transfer head heater assembly and method of transferring a micro device. U.S. Patent 16,117,414, August 30, 2018.

[36] Choi, M.; Jang, B.; Lee, W.; Lee, S.; Kim, T. W.; Lee, H. J.; Kim, J. H.; Ahn, J. H. Stretchable active matrix inorganic light-emitting diode display enabled by overlay-aligned roll-transfer printing. *Adv. Funct. Mater.* **2017**, *27*, 1606005.

[37] Sasaki, K.; Schuele, P. J.; Ulmer, K.; Lee, J. J. System and method for the fluidic assembly of emissive displays. U.S. Patent 10,418,527, September 17, 2019.

[38] Yeh, H. J. J.; Smith, J. S. Fluidic self-assembly for the integration of GaAs light-emitting diodes on Si substrates. *IEEE Photonics Technol. Lett.* **1994**, *6*, 706–708.

[39] Chang, W.; Kim, J.; Kim, M.; Lee, M. W.; Lim, C. H.; Kim, G.; Hwang, S.; Chang, J.; Min, Y. H.; Jeon, K. et al. Concurrent self-assembly of RGB microLEDs for next-generation displays. *Nature* **2023**, *617*, 287–291.

[40] Banks, D. P.; Grivas, C.; Mills, J. D.; Eason, R. W.; Zergioti, I. Nanodroplets deposited in microarrays by femtosecond Ti: Sapphire laser-induced forward transfer. *Appl. Phys. Lett.* **2006**, *89*, 193107.

[41] Voronenkov, V.; Bochkareva, N.; Gorbunov, R.; Zubrilov, A.; Kogotkov, V.; Latyshev, P.; Lelikov, Y.; Leonidov, A.; Shreter, Y. Laser slicing: A thin film lift-off method for GaN-on-GaN technology. *Results Phys.* **2019**, *13*, 102233.

[42] Kelly, M. K.; Vaudo, R. P.; Phanse, V. M.; Görgens, L.; Ambacher O.; Stutzmann, M. Large free-standing GaN substrates by hydride vapor phase epitaxy and laser-induced liftoff. *Jpn. J. Appl. Phys.* **1999**, *38*, L217–L219.

[43] Lai, S. Q.; Liu, S. B.; Li, Z. L.; Zhang, Z. N.; Chen, Z.; Zhang, R.; Kuo H. C.; Wu, T. Z. Applications of lasers: A promising route toward low-cost fabrication of high-efficiency full-color micro-LED displays. *Opto-Electron. Sci.* **2023**, *2*, 230028.

[44] Marinov, V. R. 52-4: Laser-enabled extremely-high rate technology for µLED assembly. *SID Symp. Dig. Tech. Pap.* **2018**, *49*, 692–695.

[45] Huang, J. H.; Li, Z. W.; Zhu, Y. L.; Yang, L. L.; Lin, X.; Li, Y.; Wang, Y. Z.; Wang, Y. Z.; Fu, Y.; Xu, W. D. et al. Monolithic integration of full-color microdisplay screen with Sub-5 µm quantum-dot pixels. *Adv. Mater.* **2024**, *36*, 2409025.

[46] Virey, E. H.; Baron, N.; Bouhamri, Z. 30-4: MicroLED display technology trends and intellectual property landscape. *SID Symp. Dig. Tech. Pap.* **2020**, *51*, 436–439.

[47] Fang, M. H.; Bao, Z.; Huang, W. T.; Liu, R. S. Evolutionary generation of phosphor materials and their progress in future applications for light-emitting diodes. *Chem. Rev.* **2022**, *122*, 11474–11513.

[48] Srivastava, S.; Lee, K. E.; Fitzgerald, E. A.; Pennycook, S. J.; Gradečak, S. Freestanding high-resolution quantum dot color converters with small pixel sizes. *ACS Appl. Mater. Interfaces* **2022**, *14*, 48995–49002.

[49] He, M. D.; Zhang, Q. G.; Carulli, F.; Erroi, A.; Wei, W. Y.; Kong, L.; Yuan, C. W.; Wan, Q.; Liu, M. M.; Liao, X. R. et al. Ultra-stable, solution-processable $CsPbBr_3$-SiO_2 nanospheres for highly efficient color conversion in micro light-emitting diodes. *ACS Energy Lett.* **2023**, *8*, 151–158.

[50] Murray, C. B.; Norris, D J.; Bawendi, M. G. Synthesis and characterization of nearly monodisperse CdE (E = sulfur, selenium, tellurium) semiconductor nanocrystallites. *J. Am. Chem. Soc.* **1993**, *115*, 8706–8715.

[51] Dibbell, R. S.; Watson, D. F. Distance-dependent electron transfer in tethered assemblies of CdS quantum Dots and TiO_2 nanoparticles. *J. Phys. Chem. C* **2009**, *113*, 3139–3149.

[52] Grimsdale, A. C.; Chan, K. L.; Martin, R. E.; Jokisz, P. G.; Holmes, A. B. Synthesis of light-emitting conjugated polymers for applications in electroluminescent devices. *Chem. Rev.* **2009**, *109*, 897–1091.

[53] Cao, F.; Shi, W. D.; Zhao, L. J.; Song, S. Y.; Yang, J. H.; Lei, Y. Q.; Zhang, H. J. Hydrothermal synthesis and high photocatalytic activity of 3D wurtzite ZnSe hierarchical nanostructures. *J. Phys. Chem. C* **2008**, *112*, 17095–17101.

[54] Shi, C. M.; Zhu, Y.; Cerwinka, W. H.; Zhau, H. E.; Marshall, F. F.; Simons, J. W.; Nie, S. M.; Chung, L. W. K. Quantum dots: Emerging applications in urologic oncology. *Urol. Oncol.: Semin. Orig. Invest.* **2008**, *26*, 86–92.

[55] García de Arquer, F. P.; Talapin, D. V.; Klimov, V. I.; Arakawa, Y.; Bayer, M.; Sargent, E. H. Semiconductor quantum dots: Technological progress and future challenges. *Science,* **2021**, *373*, eaaz8541.

[56] Jung, T.; Choi, J. H.; Jang, S. H.; Han, S. J. 32-1: Invited paper: Review of micro-light-emitting-diode technology for micro-display applications. *SID Symp. Dig. Tech. Pap.* **2019**, *50*, 442–446.

[57] Chen, E. G.; Lin, J. Y.; Yang, T.; Chen, Y.; Zhang, X.; Ye, Y.; Sun, J.; Yan, Q.; Guo, T. L. Asymmetric quantum-dot pixelation for color-converted white balance. *ACS Photonics* **2021**, *8*, 2158–2165.

[58] Singh, M.; Haverinen, H. M.; Dhagat, P.; Jabbour, G. E. Inkjet printing-process and its applications. *Adv. Mater.* **2010**, *22*, 673–685.

[59] Zhang, P. P.; Yang, G. L.; Kang, G. G.; Shi, J. B.; Zhong, H. Z. Photolithography of colloidal quantum dots for display applications. *Chin. J. Appl. Chem.* **2021**, *38*, 1175–1188.

[60] Kim, T. H.; Cho, K. S.; Lee, E. K.; Lee, S. J.; Chae, J.; Kim, J. W.; Kim, D. H.; Kwon, J. Y.; Amaratunga, G.; Lee, S. Y. et al. Full-colour quantum dot displays fabricated by transfer printing. *Nat. Photonics* **2011**, *5*, 176–182.

[61] Haverinen, H. M.; Myllylä, R. A.; Jabbour, G. E. Inkjet printed RGB quantum dot-hybrid LED. *J. Disp. Technol.* **2010**, *6*, 87–89.

[62] Haverinen, H. M.; Myllylä, R. A.; Jabbour, G. E. Inkjet printing of light emitting quantum dots. *Appl. Phys. Lett.* **2009**, *94*, 073108.

[63] Wilkinson, N. J.; Smith, M. A. A.; Kay, R. W.; Harris, R. A. A review of aerosol jet printing-a non-traditional hybrid process for micro-manufacturing. *Int. J. Adv. Manuf. Technol.* **2019**, *105*, 4599–4619.

[64] Hoey, J. M.; Lutfurakhmanov, A.; Schulz, D. L.; Akhatov, I. S. A review on aerosol-based direct-write and its applications for microelectronics. *J. Nanotechnol.* **2012**, *2012*, 324380.

[65] Seifert, T.; Sowade, E.; Roscher, F.; Wiemer, M.; Gessner, T.; Baumann, R. R. Additive manufacturing technologies compared: Morphology of deposits of silver ink using inkjet and aerosol jet printing. *Ind. Eng. Chem. Res.* **2015**, *54*, 769–779.

[66] Li, H. G.; Duan, Y. Q.; Shao, Z. L.; Zhang, G. N.; Li, H. Y.; Huang, Y. A.; Yin, Z. P. High-Resolution pixelated light emitting diodes based on electrohydrodynamic printing and coffee-ring-free quantum dot film. *Adv. Mater. Technol.* **2020**, *5*, 2000401.

[67] Zhu, M. H.; Duan, Y. Q.; Liu, N.; Li, H. G.; Li, J. H.; Du, P. P.; Tan, Z. F.; Niu, G. D.; Gao, L.; Huang, Y. A. et al. Electrohydrodynamically printed high-resolution full-color hybrid perovskites. *Adv. Funct. Mater.* **2019**, *29*, 1903294.

[68] Kim, B. H.; Onses, M. S.; Lim, J. B.; Nam, S.; Oh, N.; Kim, H.; Yu, K. J.; Lee, J. W.; Kim, J. H.; Kang, S. K. et al. High-resolution patterns of quantum dots formed by electrohydrodynamic jet printing for light-emitting diodes. *Nano Lett.* **2015**, *15*, 969–973.

[69] Li, Y.; Chen, Z. W.; Liang, D.; Zang, J. Q.; Song, Z. H.; Cai, L.;

Zou, Y. T.; Wang, X. C.; Wang, Y. S.; Li, P. D. et al. Coffee-stain-free perovskite film for efficient printed light-emitting diode. *Adv. Opt. Mater.* **2021**, *9*, 2100553.

[70] Lin, S. Y.; Tan, G. J.; Yu, J. H.; Chen, E. G.; Weng, Y. L.; Zhou, X. T.; Xu, S.; Ye, Y.; Yan, Q. F.; Guo, T. L. Multi-primary-color quantum-dot down-converting films for display applications. *Opt. Express* **2019**, *27*, 28480–28493.

[71] Park, J. S.; Kyhm, J.; Kim, H. H.; Jeong, S.; Kang, J.; Lee, S. E.; Lee, K. T.; Park, K.; Barange, N.; Han, J. et al. Alternative patterning process for realization of large-area, full-color, active quantum dot display. *Nano Lett.* **2016**, *16*, 6946–6953.

[72] Zou, C.; Chang, C.; Sun, D.; Bo̎hringer, K. F.; Lin, L. Y. Photolithographic patterning of perovskite thin films for multicolor display applications. *Nano Lett.* **2020**, *20*, 3710–3717.

[73] Wang, Y. Y.; Pan, J. A.; Wu, H. Q.; Talapin, D. V. Direct wavelength-selective optical and electron-beam lithography of functional inorganic nanomaterials. *ACS Nano* **2019**, *13*, 13917–13931.

[74] Lin, C. H.; Zeng, Q. J.; Lafalce, E.; Yu, S. T.; Smith, M. J.; Yoon, Y. J.; Chang, Y. J.; Jiang, Y.; Lin, Z. Q.; Vardeny, Z. V. et al. Large-area lasing and multicolor perovskite quantum dot patterns. *Adv. Opt. Mater.* **2018**, *6*, 1800474.

[75] Mei, W. H.; Zhang, Z. Q.; Zhang, A. D.; Li, D.; Zhang, X. Y.; Wang, H. W.; Chen, Z.; Li, Y. Z.; Li, X. G.; Xu, X. G. High-resolution, full-color quantum dot light-emitting diode display fabricated via photolithography approach. *Nano Res.* **2020**, *13*, 2485–2491.

[76] Kim, H. M.; Ryu, M.; Cha, J. H. J.; Kim, H. S.; Jeong, T.; Jang, J. Ten micrometer pixel, quantum dots color conversion layer for high resolution and full color active matrix micro-LED display. *J. Soc. Inf. Disp.* **2019**, *27*, 347–353.

[77] Chini, S. F.; Amirfazli, A. Understanding pattern collapse in photolithography process due to capillary forces. *Langmuir* **2010**, *26*, 13707–13714.

[78] Cho, H.; Pan, J. A.; Wu, H. Q.; Lan, X. Z.; Coropceanu, I.; Wang, Y. Y.; Cho, W.; Hill, E. A.; Anderson, J. S.; Talapin, D. V. Direct optical patterning of quantum dot light-emitting diodes via *in situ* ligand exchange. *Adv. Mater.* **2020**, *32*, 2003805.

[79] Yang, J.; Hahm, D.; Kim, K.; Rhee, S.; Lee, M.; Kim, S.; Chang, J. H.; Park, H. W.; Lim, J.; Lee, M. et al. High-resolution patterning of colloidal quantum dots via non-destructive, light-driven ligand crosslinking. *Nat. Commun.* **2020**, *11*, 2874.

[80] Wang, Y. K.; Long, R.; Yang, Y.; Zhang, D. L.; Zhang, J. B. Highly luminescent and uniform patterned quantum dot color converters via ligand engineering. *Giant* **2023**, *16*, 100202.

[81] Na, Y. J.; Park, S. J.; Lee, S. W.; Kim, J. S. Photolithographic process for the patterning of quantum dots. *Ultramicroscopy* **2008**, *108*, 1297–1301.

[82] Boles, M. A.; Ling, D. S.; Hyeon, T.; Talapin, D. V. The surface science of nanocrystals. *Nat. Mater.* **2016**, *15*, 141–153.

[83] Tang, X.; Tang, X. B.; Lai, K. W. C. Scalable fabrication of infrared detectors with multispectral photoresponse based on patterned colloidal quantum dot films. *ACS Photonics* **2016**, *3*, 2396–2404.

[84] Kovalenko, M. V.; Bodnarchuk, M. I.; Zaumseil, J.; Lee, J. S.; Talapin, D. V. Expanding the chemical versatility of colloidal nanocrystals capped with molecular metal chalcogenide ligands. *J. Am. Chem. Soc.* **2010**, *132*, 10085–10092.

[85] Fan, X. T.; Yang, X.; Kong, X. M.; Zhang, T. Q.; Wang, S. L.; Lin, Y.; Chen, Z. Recent progresses on perovskite quantum dots patterning techniques for color conversion layer in micro-LED displays. *Next Nanotechnol.* **2024**, *5*, 100045.

[86] Zhang, P. P.; Yang, G. L.; Li, F.; Shi, J. B.; Zhong, H. Z. Direct *in situ* photolithography of perovskite quantum dots based on photocatalysis of lead bromide complexes. *Nat. Commun.* **2022**, *13*, 6713.

[87] Liu, S. H.; Liu, W. B.; Ji, W. Y.; Yu, J.; Zhang, W.; Zhang, L. T.; Xie, W. F. Top-emitting quantum dots light-emitting devices employing microcontact printing with electricfield-independent emission. *Sci. Rep.* **2016**, *6*, 22530.

[88] Kim, B. H.; Nam, S.; Oh, N.; Cho, S. Y.; Yu, K. J.; Lee, C. H.; Zhang, J. Q.; Deshpande, K.; Trefonas, P.; Kim, J. H. et al. Multilayer transfer printing for pixelated, multicolor quantum dot light-emitting diodes. *ACS Nano* **2016**, *10*, 4920–4925.

[89] Choi, M. K.; Yang, J.; Kang, K.; Kim, D. C.; Choi, C.; Park, C.; Kim, S. J.; Chae, S. I.; Kim, T. H.; Kim, J. H. et al. Wearable red-green-blue quantum dot light-emitting diode array using high-resolution intaglio transfer printing. *Nat. Commun.* **2015**, *6*, 7149.

[90] Nam, T. W.; Kim, M.; Wang, Y. M.; Kim, G. Y.; Choi, W.; Lim, H.; Song, K. M.; Choi, M. J.; Jeon, D. Y.; Grossman, J. C. et al. Thermodynamic-driven polychromatic quantum dot patterning for light-emitting diodes beyond eye-limiting resolution. *Nat. Commun.* **2020**, *11*, 3040.

[91] Sun, W. C.; Li, F.; Tao, J.; Li, P. Y.; Zhu, L. C.; Li, J. W.; Lv, J. G.; Wang, W. B.; Liang, J. Q.; Zhong, H. Z. Micropore filling fabrication of high resolution patterned PQDs with a pixel size less than 5 μm. *Nanoscale* **2022**, *14*, 5994–5998.

[92] Zhao, J. Y.; Chen, L. X.; Li, D. Z.; Shi, Z. Q.; Liu, P.; Yao, Z. L.; Yang, H. C.; Zou, T. Y.; Zhao, B.; Zhang, X. et al. Large-area patterning of full-color quantum dot arrays beyond 1000 pixels per inch by selective electrophoretic deposition. *Nat. Commun.* **2021**, *12*, 4603.

[93] Kong, Y. L.; Tamargo, I. A.; Kim, H.; Johnson, B. N.; Gupta, M. K.; Koh, T. W.; Chin, H. A.; Steingart, D. A.; Rand, B. P.; McAlpine, M. C. Correction to 3D printed quantum dot light-emitting diodes. *Nano. Lett.* **2019**, *19*, 2187–2187.

[94] Kong, Y. L.; Tamargo, I. A.; Kim, H.; Johnson, B. N.; Gupta, M. K.; Koh, T. W.; Chin, H. A.; Steingart, D. A.; Rand, B. P.; McAlpine, M. C. 3D printed quantum dot light-emitting diodes. *Nano Lett.* **2014**, *14*, 7017–7023.

[95] Liu, S. F.; Hou, Z. W.; Lin, L. H.; Li, F.; Zhao, Y.; Li, X. Z.; Zhang, H.; Fang, H. H.; Li, Z. C.; Sun, H. B. 3D nanoprinting of semiconductor quantum dots by photoexcitation-induced chemical bonding. *Science* **2022**, *377*, 1112–1116.

[96] Xu, R. R.; Yin, Q. X.; You, J. Y.; Wang, X. T.; Li, M. L.; Huang, X. L.; Chen, J.; Zeng, H. B. Laser *in situ* synthesis of wide bandgap tunable perovskite and its application in micro-LEDs. *Adv. Opt. Mater.*, in press, DOI: 10.1002/adom.202403132.

[97] Maeng, S.; Park, S. J.; Lee, J.; Lee, H.; Choi, J.; Kang, J. K.; Cho, H. Direct photocatalytic patterning of colloidal emissive nanomaterials. *Sci. Adv.* **2023**, *9*, eadi6950.

[98] Yang, J.; Lee, M.; Park, S. Y.; Park, M.; Kim, J.; Sitapure, N.; Hahm, D.; Rhee, S.; Lee, D.; Jo, H. et al. Nondestructive photopatterning of heavy-metal-free quantum dots. *Adv. Mater.* **2022**, *34*, 2205504.

[99] Lee, Y.; Shin, J.; Shin, S.; Kim, E. A.; Lee, J. Y.; Gwak, N.; Kim, S.; Seo, J.; Kong, H.; Yeo, D. et al. Ring-opening polymerization of surface ligands enables versatile optical patterning and form factor flexibility in quantum dot assemblies. *Adv. Mater.* **2025**, *37*, 2415436.

[100] Tian, W. Y.; Wu, T. X.; Wu, Y. S.; Xiao, J. Q.; Wang, P. K.; Li, J. H. Application of InP quantum dot film by photolithography technology on a micro-LED display. *ECS J. Solid State Sci. Technol.* **2023**, *12*, 046003.

[101] Gong, T.; Xuan, T. T.; Bai, W. H.; Dong, H. R.; Huang, K.; Xie, R. J. Quantum dot luminescence microspheres enable ultra-efficient and bright micro-LEDs. *Adv. Mater.* **2025**, *37*, 2411999.

[102] Chu, S. Y.; Wang, H. Y.; Lee, C. T.; Lee, H. Y.; Laing, K. L.; Kuo, W. H.; Fang, Y. H.; Lin, C. C. Improved color purity of monolithic full color micro-LEDs using distributed bragg reflector and blue light absorption material. *Coatings* **2020**, *10*, 436.

[103] Krishnan, C.; Brossard, M.; Lee, K. Y.; Huang, J. K.; Lin, C. H.; Kuo, H. C.; Charlton, M. D. B.; Lagoudakis, P. G. Hybrid photonic crystal light-emitting diode renders 123% color conversion effective

quantum yield. *Optica* **2016**, *3*, 503–509.
[104] Song, J.; Kang, J. H.; Han, J. Monolithic RGB micro-light-emitting diodes fabricated with quantum dots embedded inside nanoporous GaN. *ACS Appl. Electron. Mater.* **2021**, *3*, 4877–4881.
[105] Chen, C. H.; Kuo, S. Y.; Feng, H. Y.; Li, Z. H.; Yang, S. B.; Wu, S. H.; Hsieh, H. Y.; Lin, Y. S.; Lee, Y. C.; Chen, W. C. et al. Photon color conversion enhancement of colloidal quantum dots inserted into a subsurface laterally-extended GaN nano-porous structure in an InGaN/GaN quantum-well template. *Opt. Express* **2023**, *31*, 6327–6341.
[106] Yang, S. B.; Feng, H. Y.; Lin, Y. S.; Chen, W. C.; Kuo, Y.; Yang, C. C. Effects of surface plasmon coupling on the color conversion of an InGaN/GaN quantum-well structure into colloidal quantum dots inserted into a nearby porous Structure. *Nanomaterials* **2023**, *13*, 328.
[107] Theobald, D.; Yu, S. D.; Gomard, G.; Lemmer, U. Design of selective reflectors utilizing multiple scattering by core–shell nanoparticles for color conversion films. *ACS Photonics* **2020**, *7*, 1452–1460.
[108] Lee, T. Y.; Miao, W. C.; Hung, Y. Y.; Bai, Y. H.; Chen, P. T.; Huang, W. T.; Chen, K. A.; Lin, C. C.; Chen, F. C.; Hong, Y. H. et al. Ameliorating uniformity and color conversion efficiency in quantum dot-based micro-LED displays through blue-UV Hybrid Structures. *Nanomaterials* **2023**, *13*, 2099.
[109] Zhan, T.; Yin, K.; Xiong, J. H.; He, Z. Q.; Wu, S. T. Augmented reality and virtual reality displays: Perspectives and challenges. *iScience* **2020**, *23*, 101397.
[110] Quesnel, E.; Lagrange, A.; Vigier, M.; Consonni, M.; Tournaire, M.; Le Marchand, V.; Suhm, A.; Demars, P.; Pillet, J. C.; Ben Bakir, B. et al. Dimensioning a full color LED microdisplay for augmented reality headset in a very bright environment. *J. Soc. Inf. Disp.* **2021**, *29*, 3–16.
[111] Moon, H.; Lee, C.; Lee, W.; Kim, J.; Chae, H. Stability of quantum dots, quantum dot films, and quantum dot light-emitting diodes for display applications. *Adv. Mater.* **2019**, *31*, 1804294.
[112] Pechstedt, K.; Whittle, T.; Baumberg, J.; Melvin, T. Photoluminescence of colloidal CdSe/ZnS quantum dots: The critical effect of water molecules. *J. Phys. Chem. C* **2010**, *114*, 12069–12077.
[113] Carrillo-Carrión, C.; Cárdenas, S.; Simonet, B. M.; Valcárcel, M. Quantum dots luminescence enhancement due to illumination with UV/Vis light. *Chem. Commun.* **2009**, 5214–5226.
[114] Zhang, J. K.; Li, J. Z.; Ye, Z. K.; Cui, J. T.; Peng, X. G. Hot-Electron-induced photochemical properties of CdSe/ZnSe core/shell quantum dots under an ambient environment. *J. Am. Chem. Soc.* **2023**, *145*, 13938–13949.
[115] Hu, Z.; Shu, Y. F.; Qin, H. Y.; Hu, X. F.; Peng, X. G. Water effects on colloidal semiconductor nanocrystals: Correlation of photophysics and photochemistry. *J. Am. Chem. Soc.* **2021**, *143*, 18721–18732.
[116] Zhao, Y. M.; Riemersma, C.; Pietra, F.; Koole, R.; de Mello Donegá, C.; Meijerink, A. High-temperature luminescence quenching of colloidal quantum dots. *ACS Nano* **2012**, *6*, 9058–9067.
[117] Cai, X. C.; Martin, J. E.; Shea-Rohwer, L. E.; Gong, K.; Kelley, D. F. Thermal quenching mechanisms in II-VI semiconductor nanocrystals. *J. Phys. Chem. C* **2013**, *117*, 7902–7913.
[118] Rowland, C. E.; Liu, W. Y.; Hannah, D. C.; Chan, M. K. Y.; Talapin, D. V.; Schaller, R. D. Thermal stability of colloidal InP nanocrystals: Small inorganic ligands boost high-temperature photoluminescence. *ACS Nano* **2014**, *8*, 977–985.
[119] Wang, Y. K.; Wan, H. Y.; Teale, S.; Grater, L.; Zhao, F.; Zhang, Z. D.; Duan, H. W.; Imran, M.; Wang, S. D.; Hoogland, S. et al. Long-range order enabled stability in quantum dot light-emitting diodes. *Nature* **2024**, *629*, 586–591.
[120] Zhang, J. K.; Li, C. Y.; Li, J. Z.; Peng, X. G. Synthesis of CdSe/ZnSe core/shell and CdSe/ZnSe/ZnS core/shell/shell nanocrystals: Surface-ligand strain and CdSe-ZnSe lattice strain. *Chem. Mater.* **2023**, *35*, 7049–7059.
[121] Zhang, C.; Zhuang, Y. Z.; Zhang, X. Functional adhesive and preparation method, quantum dot functional adhesive and preparation method. CN 114058298A, February 18, 2022.
[122] Wang, A. Q.; Shen, H. B.; Zang, S. P.; Lin, Q. L.; Wang, H. Z.; Qian, L.; Niu, J. Z.; Li, L. S. Bright, efficient, and color-stable violet ZnSe-based quantum dot light-emitting diodes. *Nanoscale* **2015**, *7*, 2951–2959.
[123] Kim, T.; Kim, K. H.; Kim, S.; Choi, S. M.; Jang, H.; Seo, H. K.; Lee, H.; Chung, D. Y.; Jang, E. Efficient and stable blue quantum dot light-emitting diode. *Nature* **2020**, *586*, 385–389.
[124] Wu, Z. H.; Liu, P.; Zhang, W. D.; Wang, K.; Sun, X. W. Development of InP quantum dot-based light-emitting diodes. *ACS Energy Lett.* **2020**, *5*, 1095–1106.
[125] Chen, Y. R.; Wang, R. X.; Kuang, Y. M.; Bian, Y. Y.; Chen, F.; Shen, H. B.; Chi, Z.; Ran, X.; Guo, L. J. Suppressed Auger recombination and enhanced emission of InP/ZnSe/ZnS quantum dots through inner shell manipulation. *Nanoscale* **2023**, *15*, 18920–18927.